THE ASTROPHYSICAL JOURNAL, 320:238–257, 1987 September 1

THE *IRAS* BRIGHT GALAXY SAMPLE. II. THE SAMPLE AND LUMINOSITY FUNCTION

B. T. SOIFER,[1] D. B. SANDERS,[1] B. F. MADORE,[1,2,3] G. NEUGEBAUER,[1] G. E. DANIELSON,[4]
J. H. ELIAS,[1] CAROL J. LONSDALE,[5] AND W. L. RICE[5]

Received 1986 December 1; accepted 1987 February 13

ABSTRACT

A complete sample of 324 extragalactic objects with 60 μm flux densities greater than 5.4 Jy has been selected from the *IRAS* catalogs. Only one of these objects can be classified morphologically as a Seyfert nucleus; the others are all galaxies. The median distance of the galaxies in the sample is $\sim$30 Mpc, and the median luminosity $\nu L_\nu(60\ \mu\text{m})$ is $\sim 2 \times 10^{10}\ L_\odot$. This infrared selected sample is much more "infrared active" than optically selected galaxy samples.

The range in far-infrared luminosities of the galaxies in the sample is $10^8\ L_\odot$–$2 \times 10^{12}\ L_\odot$. The far-infrared luminosities of the sample galaxies appear to be independent of the optical luminosities, suggesting a separate luminosity component. As previously found, a correlation exists between 60 μm/100 μm flux density ratio and far-infrared luminosity. The mass of interstellar dust required to produce the far-infrared radiation corresponds to a mass of gas of 10^8–$10^{10}\ M_\odot$ for normal gas to dust ratios. This is comparable to the mass of the interstellar medium in most galaxies.

The infrared luminous galaxies are found to be an important component of extraglactic objects, being the most numerous objects in the local universe at luminosities $L > 10^{11}\ L_\odot$, and producing a luminosity density of $\sim\frac{1}{4}$ that of the observed starlight in normal galaxies. Approximately 60%–80% of the far-infrared luminosity of the local universe is likely attributed to recent or ongoing star formation. If the infrared active phase ($L_{\rm FIR} > 10^{11}\ L_\odot$) is a nonrecurring event of duration less than 10^8 yr in galaxy evolution, then more than $\sim$10%, and perhaps all of the galaxies with blue luminosities greater than $10^{10}\ L_\odot$ must undergo such an event.

Subject headings: galaxies: general — infrared: general — infrared: sources — stars: formation

I. INTRODUCTION

The *IRAS* survey was the first infrared all-sky survey with sufficient sensitivity to detect a significant number of extragalactic sources. One result of the survey is the discovery that far-infrared emission dominates the total luminosity in a significant fraction of galaxies. Another, as discussed here, is the demonstration that the infrared luminous galaxies form a significant component of the local universe. To establish this, it is necessary to make a census of the galaxies that are infrared emitters, to determine the space densities of these galaxies, and to compare infrared bright galaxies with other known classes of extragalactic objects.

We have begun a study of the properties of the brightest infrared galaxies discovered in the *IRAS* survey with the goal of understanding the physical processes responsible for the infrared emission in galaxies. In this paper we describe a statistically complete sample of 324 objects selected for these studies, derive the far-infrared luminosity function of these galaxies, and compare the space densities of the *IRAS* bright galaxy sample with those of other major classes of extragalactic sources. A preliminary description of the results of the luminosity function for $L > 10^{10}\ L_\odot$ was reported by Soifer *et al.* (1986, hereafter Paper I), and a detailed description of the optical spectra and morphologies of the most luminous objects in this sample will be reported elsewhere (Sanders *et al.* 1987*a*).

II. THE *IRAS* BRIGHT GALAXY SAMPLE

The sample selected for study was designed to meet the following criteria: (1) it should be a complete sample of far-infrared–emitting extragalactic objects; (2) the size of the sample should be large enough to be able to make statistically significant statements regarding the space densities of infrared-emitting objects; (3) the objects in the sample should be accessible from northern hemisphere telescopes; and (4) the optical identifications should be made with as little ambiguity as possible. The final bright galaxy sample comprised all extragalactic objects observed by *IRAS* with 60 μm flux densities greater than 5.4 Jy, galactic latitude $|b| > 30°$, and declination $\delta > -30°$ for 0–12 hr, $\delta > -15°$ for 12–14 hr, and $\delta > -20°$ for 14–24 hr. The declination boundaries indicate areas where redshift information is complete. An extension of the bright galaxy survey to the rest of the sky covered by *IRAS* at $|b| > 30°$ and away from the Magallenic Clouds is currently under way (Elias, private communication).

For an object to be included in the *IRAS* bright galaxy sample it is necessary for it either to be identified with a cataloged extragalactic object or to have a redshift indicating it to be extragalactic. Although no morphological criteria were set for inclusion in the sample other than that there be an optical counterpart on the Palomar Sky Survey (POSS), all but one of the objects ultimately selected for inclusion in the sample are clearly extended on the POSS. The one exception to this is an

[1] Palomar Observatory, California Institute of Technology.
[2] Killam Fellow, Canada Council 1986–1988.
[3] Also at the David Dunlap Observatory, University of Toronto.
[4] Palomar Observatory and Division of Geology and Planetary Science, California Institute of Technology.
[5] IPAC, California Institute of Technology.

object with a starlike Seyfert nucleus, IRAS 0518−25 (Sanders *et al.* 1987*a*).

The total area covered by the bright galaxy survey is ~14,500 deg^2. Within the boundaries described above, small areas of the sky are not included because the *IRAS* survey coverage was insufficient for the detected sources in this area to be included in the *IRAS* catalogs. The areas omitted are described in the *IRAS Catalogs and Atlases Explanatory Supplement* (1985). The major omission in areal coverage is a gap close to the North Galactic Pole. While this is a statistically insignificant gap in the all-sky survey and in the coverage of the *IRAS* bright galaxy sample, at least two objects, NGC 4258 and NGC 4151, were detected that would have qualified, with sufficient sky coverage, for inclusion in the bright galaxy sample.

Candidate sources were generated from three *IRAS* catalogs each sampling different spatial structures: the *IRAS* Point Source Catalog (1985, hereafter the PSC) for objects with sizes less than 2′, the Small-Scale Structure Catalog (1986, hereafter the SSSC) for objects with sizes in the range 2′–8′, and the Catalog of *IRAS* Observations of Large Galaxies (Rice *et al.* 1987, hereafter LGC) for larger objects. While there is no requirement that an object appear in the PSC, all objects that qualified for inclusion in the bright galaxy sample indeed have an entry in the PSC. Several of the brighter galaxies from the PSC are also listed in the SSSC or LGC. Of the total of 324 objects in the bright galaxy sample, 289 were selected from the PSC, eight were selected based on their 60 μm flux density in the LGC, and 27 were selected from the SSSC.

Few of the objects selected from the PSC are Galactic sources. Of the 405 sources in the PSC meeting the areal and 60 μm flux density constraints, 98 have 25 μm flux densities greater than 60 μm flux densities, and all of these are associated with Galactic sources. Of the remaining 307 objects, seven sources are associated with the local group galaxy M33, two with NGC 253, and 287 represent other individual galaxies. Of the remaining 11 sources, six are planetary nebulae, two are positionally coincident with bright SAO stars, one is a peculiar galactic object, IRAS 0937+12, which is morphologically similar to the Egg Nebula (Ney *et al.* 1975; Kleinman, private communication), and two have no obvious optical counterparts. One of these latter two is in the direction of the dark nebula L1642 and can be identified with that source. The other, IRAS 1345+08, has no obvious optical counterpart, although there is a very faint stellar object within ~20″ of the *IRAS* position. No optical spectrum was obtained for this object, though it was assumed from its infrared energy distribution to be a Galactic source.

Of the objects included in the bright galaxy sample from the SSSC, all those with galaxy counterparts on the POSS have associations with previously cataloged bright galaxies. The candidate sources from the SSSC without counterparts in the PSC have neither associations with previously cataloged galaxies nor visible counterparts on the POSS, and are therefore attributed to high Galactic latitude "infrared cirrus" (Low *et al.* 1984). The existence of bright 60 μm "cirrus" that produces such reproducible signatures has been confirmed by Low (private communication). There are no sources brighter than the 5.4 Jy limit of the bright galaxy sample and selected from the SSSC that can be identified as extragalactic and do not have comparatively bright counterparts on the POSS.

The LGC represents all galaxies known to have optical diameters greater than 8′. This catalog shows only one object out of ~90 (NGC 6822) that possibly has an optical diameter less than the infrared diameter, so that the inclusion of objects from this catalog probably implies that all objects meeting the areal constraints with infrared sizes greater than 8′ are included.

III. THE DATA

The observational data for the galaxies in the bright galaxy sample are given in Table 1. Except for the large galaxies, where the positions are taken from the *Second Reference Catalogue of Bright Galaxies* (de Vaucouleurs, de Vaucouleurs, and Corwin 1976), the positions for the galaxies are from the PSC.

The total 60 μm and 100 μm flux densities are taken (in decreasing order of priority) from the LGC, the SSSC, and the PSC. This order of selection of total flux density ensures that the estimate of the largest total flux density for a given galaxy has been used. Twenty-nine galaxies in the bright galaxy sample have 60 μm flux densities taken from the LGC; 53 60 μm flux densities were obtained from the SSSC. In the case of NGC 5195, because of its proximity to M51, the 60 μm and 100 μm flux densities were estimated from one-dimensional co-addition of the *IRAS* survey data by subtracting a contribution from M51 that was assumed to be symmetrically distributed about the position of M51. Because the galaxies in this sample are all comparatively bright, the uncertainties in the reported flux densities are all dominated by systematic and calibration uncertainties, and should be less than 15%.

The flux densities reported in Table 1 have been corrected for the large bandwidths of the *IRAS* 60 μm and 100 μm filters, assuming the intrinsic spectrum to be a Planck curve multiplied by an emissivity proportional to frequency. Typically the corrections are 30%–10% at 60 μm and <2% at 100 μm. The uncertainty in the intrinsic spectrum of the source leads to an uncertainty in the correction term of roughly ±5% (see the *IRAS* Explanatory Supplement 1985).

Distances established from primary distance indicators (Sandage and Tammann 1981) or the Tully-Fisher relation (Aaronson *et al.* 1982*a*; Aaronson and Mould 1983) and modified for the distance adopted for the Virgo cluster (see below), have been adopted where available. For galaxies where neither of these are available, heliocentric radial velocities, from the literature (Palumbo, Tanzella-Nitta, and Vettolani, 1983; Huchra *et al.* 1983; Rood, private communication), were used in combination with a Hubble constant of 75 km s^{-1} Mpc^{-1}.

For those galaxies where no radial velocity was found in the literature, observations of the optical spectrum were made using the double spectrograph (Oke and Gunn 1982) on the 5 m Hale telescope of the Palomar Observatory. For these observations, the resolution was 12 Å at Hα, and the uncertainty in the radial velocity is ±300 km s^{-1}. In all cases where a galaxy redshift was determined from observations obtained at Palomar, the galaxy had strong emission lines of Hα, [N II], [O III], and Hβ. The optical spectra of these galaxies are discussed in detail by Sanders *et al.* (1987*b*).

Where distances were determined from redshifts, the distance to each galaxy was derived using the Virgocenric flow of Aaronson *et al.* (1982*b*). For all galaxies where distances were taken from the Fisher-Tully relation or the Virgocentric flow model the distances were scaled assuming Virgo is at 17.6 Mpc and the infall velocity toward Virgo is 350 km s^{-1} (i.e., H_0 = 75 km s^{-1} Mpc^{-1} at large distances). All galaxies within 6° of the center of the Virgo cluster were assumed to be members of

TABLE 1

IRAS BRIGHT GALAXY SAMPLE

NAME	RA (1950)	DEC (1950)	F_ν (Jy) 60μm	F_ν (Jy) 100μm	cz km s^{-1}	D Mpc	Log L_{fir} $L_\odot$	m_z[a] mag	Other Name
NGC 23	0^h 7^m 19^s.4	+25° 38′ 46″	9.6	16.0	4536	...	10.93	12.5	UGC 89
NGC 34	0 8 33.4	−12 23 10	17.6	17.1	5931	...	11.34	13.0	Mrk 938
MCG−02-01-051	0 16 18.0	−10 39 14	7.1	9.1	7513	...	11.16	...	Arp 256
NGC 150	0 31 47.3	−28 4 44	10.1	17.5	1593	...	9.96	12.5	
NGC 157	0 32 13.9	− 8 40 23	18.6	37.8	1651	...	10.35	11.5	
NGC 174	0 34 31.4	−29 45 11	12.1	19.2	3471	...	10.71	14.0	
NGC 232	0 40 17.5	−23 50 2	10.7	18.7	6250	...	11.23	14.0	
NGC 247	0 44 40.0	−21 2 0	10.5	30.2	...	3.6	8.67	9.8	
NGC 253	0 45 5.0	−25 33 47	1245.0	2345.0	...	3.6	10.60	7.5	
UGC 556	0 52 7.7	+28 58 26	6.1	9.9	4567	...	10.74	15.3	
NGC 337	0 57 19.9	− 7 50 53	8.6	17.2	1651	...	10.00	12.5	
IC 1623	1 5 18.0	−17 46 37	22.6	28.9	5550	...	11.38	15.5	VV114A/B
MCG−03-04-014	1 7 42.0	−17 7 1	7.7	9.9	10040	...	11.45	15.0	
NGC 470	1 17 9.6	+ 3 8 53	6.7	12.0	2374	...	10.19	12.4	UGC 858
MCG+02-04-025	1 17 22.8	+14 5 53	11.4	9.7	9337	...	11.55	14.5	
UGC 903	1 19 6.5	+17 19 52	8.4	14.4	2320	...	10.29	14.7	
NGC 520	1 21 59.5	+ 3 31 52	33.5	47.6	2261	...	10.79	12.4	UGC 966
NGC 578	1 28 03.7	−22 55 40	5.4	12.1	1696	...	9.81	11.5	
NGC 598	1 31 03.0	+30 23 54	475.0	1724.0	...	0.8	9.11	6.5	M33
NGC 613	1 31 59.0	−29 40 34	24.2	49.1	1487	...	10.31	11.0	
NGC 628	1 34 1.0	+15 31 36	22.8	65.2	655	...	9.87	10.5	M74
IRAS 0136-10	1 36 24.0	−10 42 25	7.0	6.2	14250	...	11.71	...	
NGC 660	1 40 21.6	+13 23 42	76.1	107.1	862	...	10.38	12.8	UGC 1201
III Zw 035	1 41 48.0	+16 51 7	13.8	13.3	8215	...	11.54	15.8[1]	
NGC 693	1 47 54.2	+ 5 53 53	7.9	11.0	1593	...	9.86	13.5	UGC 1304
NGC 695	1 48 28.1	+22 20 10	8.6	13.2	9769	...	11.52	13.5	UGC 1315
NGC 701	1 48 35.0	− 9 57 0	6.5	13.6	...	18.9	9.80	13.0	
UGC 1351	1 50 18.7	+12 27 43	6.6	12.3	4597	...	10.78	14.0	IC 1743
UGC 1451	1 55 41.5	+25 7 5	7.1	12.9	4916	...	10.88	14.3	
NGC 772	1 56 34.6	+18 45 52	8.1	21.0	...	33.1	10.47	11.3	Arp 78
NGC 835	2 6 56.6	−10 22 23	6.2	10.7	4066	...	10.60	13.5	Arp 318
UGC 1720	2 11 28.3	+ 4 56 28	5.6	8.2	3448	...	10.39	14.4	Mrk 1027
NGC 873	2 14 5.3	−11 34 55	6.2	12.1	3450	...	10.47	13.0	
NGC 877	2 15 15.1	+14 18 36	12.4	24.3	3866	...	10.91	12.5	UGC 1768
NGC 908	2 20 46.6	−21 27 36	14.4	44.7	1508	...	10.23	11.0	
NGC 922	2 22 49.4	−25 0 54	5.5	9.5	3086	...	10.28	12.5	
NGC 958	2 28 11.8	− 3 9 32	5.5	15.2	5750	...	11.02	11.5	
NGC 992	2 34 35.8	+20 53 6	10.7	16.6	4119	...	10.85	13.5	UGC 2103
NGC 1022	2 36 4.6	− 6 53 31	21.0	26.7	1498	...	10.18	...	
NGC 1055	2 39 11.8	+ 0 13 52	21.7	60.8	1005	...	10.08	12.5	UGC 2173
NGC 1068	2 40 7.2	− 0 13 30	188.9	238.7	1125	...	10.90	9.7	M77
NGC 1083	2 43 18.7	−15 34 5	7.7	14.1	5040	...	10.89	14.0	
NGC 1084	2 43 32.4	− 7 47 13	27.4	55.1	1402	...	10.34	12.0	
UGC 2238	2 43 33.4	+12 53 10	8.8	15.7	6250	...	11.16	15.2	
IRAS 0243+21	2 43 49.2	+21 22 44	6.2	6.5	6810	...	11.00		
NGC 1087	2 43 51.8	− 0 42 25	9.6	29.6	1503	...	10.10	11.5	UGC 2245
NGC 1134	2 50 57.1	+12 48 43	9.6	17.5	3595	...	10.72	13.2	UGC 2365
UGC 2369	2 51 15.6	+14 46 1	8.0	11.9	9354	...	11.44	14.6	
NGC 1143/4	2 52 38.6	− 0 23 6	5.6	11.4	8550	...	11.28	13.2	UGC 2388/9
UGC 2403	2 53 23.0	+ 0 29 28	7.8	11.3	5450	...	10.93	14.9	
NGC 1187	3 0 23.8	−23 3 43	10.3	23.4	1394	...	9.90	11.0	

the cluster, and their distances are taken as 17.6 Mpc. In addition the galaxies within 20° of the center of Virgo, whose distances are not derived from another source, and whose radial velocity is within 400 km s^{-1} of that of Virgo, are assumed to be cluster members. All distance and redshift information used for the bright galaxy sample is given in Table 1.

IV. COMPLETENESS OF THE SAMPLE

Because the completeness limit of the PSC at 60 μm is $\sim$0.5 Jy (*IRAS* Explanatory Supplement 1985) the *IRAS* bright galaxy sample should be highly complete. The completeness of the PSC is well understood (Chester 1986; *IRAS* Explanatory Supplement 1985). The SSSC is estimated to be complete above 10 Jy at 60 μm, although this has not been investigated in detail (SSSC Introduction, 1986). Thus there could be some incompleteness in sources selected from the SSSC for inclusion in the bright galaxy sample. This is unlikely to be significant since the differential number counts with the flux density of the sources in the bright galaxy sample in Figure 1 shows an acceptable fit to an $N \approx f_\nu^{-3/2}$ distribution to the lowest flux bin. It therefore appears that the bright galaxy sample is, to a good approximation, a complete and unbiased sample of 60 μm extragalactic sources. Note that the objects in the bright galaxy sample have been selected on the basis of

TABLE 1—*Continued*

NAME	RA (1950)	DEC (1950)	F_ν(Jy) 60μm	F_ν(Jy) 100μm	cz km s^{-1}	D Mpc	Log L_{fir} $L_\odot$	m_z[a] mag	Other Name
NGC 1204	3 2 16.8	−12 32 6	8.1	10.4	4282	...	10.70	15.0	
NGC 1222	3 6 24.2	− 3 8 49	13.2	15.3	2600	...	10.46	...	
NGC 1232	3 7 28.3	−20 45 49	10.9	40.9	1720	...	10.31	11.1	Arp 41
NGC 1266	3 13 28.6	− 2 36 43	11.7	16.6	2035	...	10.22	14.0	
NGC 1309	3 19 46.1	−15 34 34	5.7	14.0	2138	...	10.06	12.5	
IC 1953	3 31 29.5	−21 38 42	9.1	11.1	1995	...	10.03	12.5	
NGC 1377	3 34 25.7	−21 3 58	7.1	5.5	1474	...	9.66	14.0	
NGC 1385	3 35 19.7	−24 39 47	16.8	35.4	1488	...	10.15	12.0	
IRAS 0335+15	3 35 57.1	+15 23 6	5.9	7.0	10600	...	11.38	...	
NGC 1415	3 38 45.6	−22 43 30	5.6	12.1	1617	...	9.76	12.5	
NGC 1421	3 40 8.9	−13 38 49	12.1	21.7	2099	...	10.29	12.0	
NGC 1482	3 52 25.9	−20 38 53	33.1	45.6	1655	...	10.44	14.0	
UGC 2982	4 9 43.2	+ 5 25 12	8.9	16.0	5321	...	11.02	15.5	
MCG−03-12-002	4 19 6.5	−18 55 48	5.8	9.1	9477	...	11.30	15.5	
NGC 1614	4 31 35.8	− 8 40 55	34.0	31.1	4745	...	11.41	15.0	Mrk 617
IRAS 0433-25	4 33 35.0	−25 14 6	5.6	9.6	4843	...	10.70	...	
MCG−04-12-003	4 37 1.0	−24 16 52	6.3	11.2	4422	...	10.68	14.0	
NGC 1637	4 38 57.1	− 2 57 11	5.9	13.5	726	...	9.13	11.5	
NGC 1667	4 46 9.8	− 6 24 29	6.1	14.5	4600	...	10.80	...	
IRAS 0518-25	5 18 58.6	−25 24 40	13.8	11.0	12706	...	11.89	15.4[1]	
IRAS 0833+65	8 33 55.4	+65 17 49	6.2	6.5	5608	...	10.88	...	
NGC 2623	8 35 25.2	+25 55 48	25.6	27.3	5538	...	11.47	14.5	Arp 243
NGC 2633	8 42 32.9	+74 16 59	16.9	26.5	2157	...	10.65	12.5	UGC 4574
NGC 2683	8 49 35.0	+33 36 30	10.3	34.5	284	...	8.76	9.7	
NGC 2681	8 50 0.7	+51 30 4	7.5	11.0	720	...	9.48	10.4	UGC 4645
IRAS 0857+39	8 57 13.0	+39 15 40	7.2	4.2	17480	...	11.99	15.0[1]	
NGC 2748	9 8 1.0	+76 40 52	7.2	19.3	1489	...	10.20	11.7	UGC 4825
NGC 2782	9 10 54.0	+40 19 12	8.8	13.4	2552	...	10.46	12.3	Arp 215
NGC 2785	9 12 2.9	+41 7 34	9.2	16.3	2737	...	10.57	14.9	UGC 4876
UGC 4881	9 12 39.6	+44 32 20	6.3	9.9	11957	...	11.59	14.9	Arp 55
NGC 2798	9 14 11.0	+42 12 29	23.8	28.4	1755	...	10.59	12.9	UGC 4905
NGC 2820	9 17 43.2	+64 28 14	5.5	9.5	1686	...	10.02	13.1	UGC 4961
NGC 2856	9 20 53.3	+49 27 50	5.9	8.8	2638	...	10.32	13.9	Arp 285
NGC 2903	9 29 19.9	+21 43 23	59.5	154.9	554	...	9.93	9.8	UGC 5079
UGC 5101	9 32 4.6	+61 34 37	12.8	19.6	12000	...	11.90	15.5	
MCG+08-18-012	9 33 18.5	+48 41 53	6.2	8.1	7790	...	11.19	15.0	
NGC 2967	9 39 29.3	+ 0 33 58	5.4	15.0	1887	...	10.17	12.2	UGC 5180
NGC 2966	9 39 34.1	+ 4 54 7	5.7	8.0	2048	...	10.06	14.0	UGC 5181
NGC 2964	9 39 55.7	+32 4 37	12.4	23.7	1319	...	10.20	12.0	Mrk 404
NGC 2976	9 43 6.2	+68 9 22	10.7	29.6	...	3.4	8.62	10.9	UGC 5221
NGC 2990	9 43 40.6	+ 5 56 20	5.4	9.4	3155	...	10.42	12.5	UGC 5229
IC 563/4	9 43 44.2	+ 3 17 26	6.6	10.4	6100	...	11.01	14.1	Arp 303
NGC 2985	9 45 54.0	+72 30 43	5.8	19.4	1277	...	10.10	11.1	UGC 5253
NGC 3044	9 51 6.2	+ 1 48 54	9.8	20.0	1318	...	10.06	12.4	UGC 5311
NGC 3031	9 51 29.0	+69 18 4	49.0	177.7	...	3.4	9.39	8.1	M81
NGC 3034	9 51 42.5	+69 54 58	1198.4	1129.9	...	3.4	10.45	9.2	M82
NGC 3067	9 55 26.2	+32 36 32	9.6	18.9	1506	...	10.20	12.7	UGC 5351
NGC 3079	9 58 35.0	+55 55 16	45.9	89.4	...	19.2	10.63	11.2	UGC 5387
NGC 3094	9 58 42.0	+16 0 43	11.3	13.8	2388	...	10.48	13.5	UGC 5390
NGC 3077	9 59 17.0	+68 58 37	15.6	24.6	...	3.4	8.60	10.7	UGC 5398
NGC 3110	10 1 32.2	− 6 14 2	11.6	21.5	4840	...	11.10	13.5	

60 μm flux density, not total far-infrared or total infrared flux, and all statements regarding completeness apply only at 60 μm.

V. BASIC PROPERTIES OF THE BRIGHT GALAXY SAMPLE

Figure 2 shows the distribution of distances to the galaxies in the bright galaxy sample. These galaxies range in distances from 0.6 Mpc for M33 to greater than 300 Mpc for the most distant galaxies in the sample. The median distance for the galaxies in the sample, excluding Virgo galaxies, is 32 Mpc. Thus the *IRAS* bright galaxy sample extends well beyond the Local Supercluster, but is not sampling objects at distances significant with respect to the size of the universe. A total of 31 sample galaxies are identified as associated with the Virgo cluster. Thus the Virgo cluster presents a 10% contribution to the bright galaxy sample.

Histograms of the far-infrared and blue luminosities of the objects in the bright galaxy sample are plotted in Figure 3. The total far-infrared luminosity L_{FIR} for the galaxy is calculated using the far-infrared flux, f_{FIR}, which is derived by fitting the 60 μm and 100 μm flux densities to a single temperature Planck function multiplied by an emissivity $\epsilon \propto \nu$ (*Cataloged Galaxies and Quasars Observed in the IRAS Survey*, Appendix B, 1985). For luminosity calculations the deceleration constant q_0 was assumed to be zero. The blue luminosity is the quantity $\nu L_\nu(0.43\ \mu\text{m})$ and is derived from the Zwicky (blue) magnitudes given in Table 1. The blue flux, $f_b \equiv \nu f_\nu$ (0.43 μm), has been estimated from the relation between m_b and m_z suggested by

TABLE 1—*Continued*

NAME	RA (1950)	DEC (1950)	F_ν(Jy) 60μm	F_ν(Jy) 100μm	cz km s^{-1}	D Mpc	Log L_{fir} $L_\odot$	m_z[a] mag	Other Name
NGC 3166	10 11 11.8	+ 3 40 12	5.9	13.3	1381	...	9.93	11.2	UGC 5516
NGC 3169	10 11 39.6	+ 3 42 50	7.0	19.8	1205	...	9.98	11.9	UGC 5525
NGC 3147	10 12 38.4	+73 39 0	6.9	24.7	2820	...	10.74	11.3	UGC 5532
NGC 3177	10 13 48.5	+21 22 23	9.6	17.8	1303	...	10.10	12.8	UGC 5544
NGC 3184	10 15 16.4	+41 40 28	7.8	28.0	589	...	9.43	10.3	UGC 5557
NGC 3198	10 16 52.0	+45 48 00	7.4	19.2	665	...	9.52	10.7	
IRAS 1017+08	10 17 22.1	+ 8 28 41	6.1	5.4	14390	...	11.68	...	
NGC 3221	10 19 33.4	+21 49 34	7.3	18.7	3971	...	10.89	14.3	UGC 5601
NGC 3227	10 20 46.6	+20 7 8	8.2	17.3	1110	...	9.95	12.0	UGC 5620
NGC 3294	10 33 23.5	+37 34 59	6.3	17.1	1592	...	10.21	11.5	UGC 5753
NGC 3310	10 35 39.6	+53 45 50	34.8	40.7	970	...	10.39	11.0	Arp 217
NGC 3344	10 40 46.4	+25 11 07	8.9	20.1	585	...	8.98	11.8	
NGC 3351	10 41 19.0	+11 58 1	18.3	35.1	776	...	9.42	10.7	M95
NGC 3353	10 42 15.1	+56 13 30	5.4	6.4	940	...	9.57	12.9	Mrk 35
NGC 3359	10 43 21.1	+63 29 04	7.1	13.8	...	19.4	9.83	11.0	UGC 5873
NGC 3367	10 43 54.7	+14 0 58	6.1	12.8	3040	...	10.53	12.0	UGC 5880
NGC 3368	10 44 7.7	+12 4 59	9.6	27.4	899	...	9.45	12.0	M96
NGC 3395/6	10 47 4.3	+33 15 0	11.6	16.6	1630	...	10.31	12.1	Arp 270
NGC 3424	10 48 59.8	+33 9 54	9.5	17.1	1494	...	10.22	13.2	UGC 5972
NGC 3432	10 49 44.2	+36 53 26	8.0	12.4	...	10.9	9.32	11.6	Arp 206
NGC 3437	10 49 52.8	+23 12 4	12.2	20.3	1291	...	10.23	12.6	UGC 5995
NGC 3448	10 51 38.4	+54 34 19	5.9	10.9	1380	...	9.96	12.2	Arp 205
NGC 3471	10 56 2.2	+61 47 53	8.9	11.8	2254	...	10.39	13.0	Mrk 158
IRAS 1056+24	10 56 35.5	+24 48 43	12.7	13.8	12501	...	11.87	...	
NGC 3486	10 57 40.0	+29 14 44	7.0	13.5	720	...	9.06	11.1	UGC 6079
NGC 3504	11 0 28.6	+28 14 28	20.0	32.4	1549	...	10.55	11.5	UGC 6118
NGC 3508	11 0 30.7	−16 1 12	7.5	13.9	3580	...	10.66	14.0	
NGC 3511	11 0 56.2	−22 48 58	9.3	21.1	1226	...	9.94	11.5	
A1101+41	11 1 5.8	+41 7 8	6.5	10.4	10350	...	11.50	15.0	V32
NGC 3521	11 3 14.2	+ 0 14 6	50.0	130.5	804	...	9.94	10.1	UGC 6150
NGC 3556	11 8 35.3	+55 56 46	35.3	83.8	697	...	10.30	10.9	M108
NGC 3583	11 11 23.0	+48 35 17	7.3	17.7	2135	...	10.42	11.6	UGC 6263
NGC 3593	11 11 59.8	+13 5 28	20.4	35.5	621	...	9.16	11.8	UGC 6272
NGC 3597	11 12 14.4	−23 27 18	13.8	16.8	3300	...	10.77	13.0	
NGC 3627	11 17 39.6	+13 15 36	62.5	151.3	...	9.9	10.25	8.9	M66
NGC 3628	11 17 41.8	+13 51 40	54.0	127.8	...	9.9	10.18	11.5	UGC 6350
NGC 3631	11 18 12.0	+53 26 38	12.0	25.0	1161	...	10.21	11.0	Arp 27
MCG+00-29-023	11 18 38.6	− 2 42 36	5.7	8.9	7230	...	11.10	15.0	
NGC 3655	11 20 17.5	+16 51 50	7.9	18.9	1481	...	9.85	11.6	UGC 6396
NGC 3672	11 22 30.0	− 9 31 12	9.3	22.7	1855	...	10.37	12.0	
UGC 6436	11 23 9.8	+14 56 53	6.9	10.0	10216	...	11.48	15.4	IC 2810
NGC 3675	11 23 25.4	+43 51 32	12.5	35.6	771	...	9.86	10.4	UGC 6439
NGC 3683	11 24 42.7	+57 9 7	14.7	29.3	1656	...	10.49	12.7	UGC 6458
NGC 3690	11 25 42.0	+58 50 17	108.9	108.6	3159	...	11.72	11.8	Mrk 171
NGC 3726	11 30 37.3	+47 18 16	6.7	21.3	...	16.7	9.87	11.1	UGC 6537
NGC 3735	11 33 0.5	+70 48 50	7.5	17.8	2696	...	10.58	12.6	UGC 6567
NGC 3810	11 38 23.8	+11 44 53	13.0	31.4	...	17.7	10.07	11.4	UGC 6644
NGC 3877	11 43 29.5	+47 46 16	8.3	18.9	...	17.4	9.85	11.8	UGC 6745
NGC 3885	11 44 16.6	−27 38 53	11.9	14.8	1948	...	10.30	13.0	

Kirschner, Oemler, and Schechter (1978) and the absolute calibration of the blue magnitude given by Allen (1973). In all plots that follow where a blue flux is required, this conversion to the m_b system has been applied. Since one of the selection criteria for the bright galaxy sample was high galactic latitude, extinction in the blue has been neglected, as have corrections for inclination or internal reddening.

The range of observed far-infrared luminosities extends from $\sim 10^8\ L_\odot$ to greater than $10^{12}\ L_\odot$, with the mode of the distribution occurring at $\sim 2 \times 10^{10}\ L_\odot$. A similar distribution (adjusted to the same Hubble constant) was found by Lawrence *et al.* 1986. All the sources in the bright galaxy sample have far-infrared flux densities much greater than can be attributed directly to a stellar population, while none are known radio-loud objects where the infrared emission could be expected to be an extension of the radio nonthermal emission. Furthermore, many of the objects in the sample show spatial extent at 60 μm. Thus, we assume that the far-infrared peak in the energy distribution is due to thermal emission by dust. For far-infrared luminosities of $\sim 2 \times 10^{10}\ L_\odot$ and typical dust temperatures of ~ 35 K, the mass of dust required to produce the observed luminosity is $\sim 4 \times 10^6\ M_\odot$ assuming optically thin dust emission and normal dust parameters (e.g., Draine and Lee 1984). This corresponds to a total gas mass of $\sim 10^9\ M_\odot$, quite typical for the interstellar medium of large spiral galaxies.

As can be seen from Figure 3 the mean blue luminosity is significantly lower than the far-infrared luminosity, while the dispersion in the blue luminosities is about half that in the far-infrared luminosities. For the 312 galaxies with blue

TABLE 1—*Continued*

NAME	RA (1950)	DEC (1950)	F_ν(Jy) 60μm	F_ν(Jy) 100μm	cz km s^{-1}	D Mpc	Log L_{fir} $L_\odot$	m_z[a] mag	Other Name
NGC 3887	11 44 31.9	−16 34 26	7.7	15.4	1130	...	9.80	11.6	
NGC 3893	11 46 0.0	+48 59 20	14.5	34.9	977	...	10.22	10.6	UGC 6778
NGC 3938	11 50 12.8	+44 23 58	9.0	21.5	792	...	9.71	11.0	UGC 6856
NGC 3949	11 51 5.0	+48 8 13	11.2	25.0	804	...	9.89	10.9	UGC 6869
NGC 3953	11 51 11.8	+52 36 25	7.1	36.4	...	20.2	10.24	10.8	UGC 6870
NGC 3955	11 51 24.2	−22 53 10	8.4	17.4	1345	...	10.01	12.0	
NGC 3981	11 53 35.5	−19 37 23	6.6	18.8	1717	...	10.22	12.5	Arp 289
NGC 3994	11 55 5.7	+32 34 11	9.8	21.1	3250	...	10.82	12.8	UGC 6944
NGC 3982	11 53 51.8	+55 24 11	7.2	15.8	1110	...	9.98	12.4	
NGC 4013	11 55 55.9	+44 13 34	8.4	21.6	835	...	9.84	12.4	
NGC 4027	11 56 56.9	−18 59 13	10.8	27.9	1677	...	10.40	11.6	Arp 22
NGC 4030	11 57 49.4	− 0 49 16	17.5	46.4	1463	...	10.26	12.4	UGC 6993
NGC 4038/9	11 59 19.4	−18 35 53	41.6	76.0	1563	...	10.81	10.5	Arp 244
NGC 4041	11 59 38.9	+62 24 54	14.5	31.3	1234	...	10.34	11.6	UGC 7014
NGC 4045	12 0 7.9	+ 2 15 22	7.1	13.6	1995	...	10.28	13.5	UGC 7021
NGC 4051	12 0 36.0	+44 48 36	11.2	20.8	710	...	9.53	11.2	
NGC 4085	12 2 49.2	+50 37 59	5.8	14.5	751	...	9.61	12.8	UGC 7075
NGC 4088	12 3 1.7	+50 49 5	25.1	51.9	763	...	10.19	11.2	Arp 18
NGC 4096	12 3 28.5	+47 45 26	7.8	19.7	...	11.1	9.49	11.6	
NGC 4100	12 3 36.2	+49 51 40	9.0	20.7	1076	...	10.08	11.7	UGC 7095
NGC 4102	12 3 50.9	+52 59 20	49.9	67.3	863	...	10.52	11.8	UGC 7096
NGC 4123	12 5 37.4	+ 3 9 25	6.2	10.8	...	18.0	9.68	13.1	UGC 7116
NGC 4157	12 8 34.6	+50 45 40	19.1	43.7	771	...	10.11	11.9	UGC 7183
NGC 4174	12 9 58.8	+29 26 46	5.7	11.0	4061	...	10.71	14.2	UGC 7211
IRAS 1211+03	12 11 12.2	+ 3 5 20	8.8	9.5	21703	...	12.19	16.9[1]	
NGC 4192	12 11 16.1	+15 10 34	8.8	26.4	...	12.4	9.68	11.0	M98
NGC 4194	12 11 41.3	+54 48 11	23.4	25.0	2528	...	10.87	13.0	
NGC 4212	12 13 2.6	+14 11 10	7.0	16.4	2125	...	9.79	11.9	UGC 7275
NGC 4214	12 13 9.4	+36 36 4	16.5	29.2	288	...	8.70	10.3	
NGC 4254	12 16 17.3	+14 41 38	35.2	73.2	2447	...	10.47	10.2	M99
NGC 4273	12 17 22.3	+ 5 37 16	10.4	21.5	2375	...	10.60	12.3	UGC 7380
NGC 4298	12 19 3.6	+14 52 44	6.7	19.1	1116	...	9.85	12.1	UGC 7412
NGC 4303	12 19 24.0	+ 4 44 53	35.2	61.8	1568	...	10.85	10.9	M61
NGC 4321	12 20 24.7	+16 5 46	23.4	58.1	1576	...	10.33	10.6	M100
NGC 4332	12 20 27.1	+66 7 12	8.0	14.0	2843	...	10.57	13.2	UGC 7453
NGC 4369	12 22 8.2	+39 39 32	6.3	11.3	1052	...	9.88	12.3	Mrk 439
IRAS 1222-06	12 22 29.0	− 6 24 14	6.4	7.5	7495	...	11.14	...	
NGC 4383	12 22 53.0	+16 44 53	9.1	12.0	1695	...	9.77	12.3	UGC 7507
NGC 4388	12 23 14.4	+12 56 24	11.1	17.4	...	18.8	9.94	12.2	UGC 7520
NGC 4395	12 23 20.0	+33 49 30	5.7	13.4	294	...	8.29	11.7	
NGC 4402	12 23 35.3	+13 23 24	6.0	17.4	242	...	9.81	13.6	UGC 7528
NGC 4414	12 23 57.8	+31 29 56	27.6	68.6	...	13.0	10.14	10.9	UGC 7539
NGC 4418	12 24 22.1	− 0 36 14	43.7	32.0	2045	...	11.00	14.2	UGC 7545
NGC 4419	12 24 24.5	+15 19 26	8.1	17.7	37	...	9.84	11.6	UGC 7551
NGC 4433	12 25 4.6	− 8 0 14	14.1	25.6	2978	...	10.82	13.0	
NGC 4438	12 25 14.0	+13 17 06	5.5	15.5	259	...	9.77	12.0	
NGC 4490	12 28 8.2	+41 55 23	42.5	78.1	577	...	9.80	10.1	UGC 7651
NGC 4501	12 29 28.1	+14 41 28	16.7	56.2	...	17.5	10.32	10.6	M88
NGC 4526	12 31 30.7	+ 7 58 26	6.2	15.8	447	...	9.80	10.6	UGC 7718
NGC 4527	12 31 35.0	+ 2 55 48	27.3	63.7	1737	...	10.87	12.4	UGC 7721

magnitudes given in Table 1 $\sigma[\log(L_b)] = 0.43$, while $\sigma[\log(L_{FIR})] = 0.70$ for all 324 galaxies in the sample.

The objects in the bright galaxy sample are, not surprisingly, more "infrared active" than those in an optical magnitude limited sample detected in the *IRAS* survey. This is illustrated in Figure 4, where histograms of far-infrared to blue flux ratios are plotted for the bright galaxy sample and for the galaxies brighter than 14.5 mag in the UGC catalog (Nilson 1973; Rice, private communication) that have *IRAS* detections.

For the infrared-selected sample the values of $\log(f_{FIR}/f_b)$ range from −0.9 to 2.1, while the range for the optically selected sample is −1.5 to 2.1. The median value of $\log(f_{FIR}/f_b)$ for the *IRAS* galaxies is ∼0.4, while for the optical sample the median value is ∼ −0.2. Note that the UGC galaxies without *IRAS* detections will have $\log(f_{FIR}/f_b) < 0$. Since only half of the UGC galaxies with $m_b < 14.5$ mag are detected by *IRAS*, the median value of $\log(f_{FIR}/f_b)$ for an optically selected sample with infrared measurements for all sources must be still smaller. From Figure 4 it is clear that the infrared flux-limited sample consists of galaxies with much greater average infrared luminosity than does the optically selected sample.

Figure 5*a* shows that f_{FIR}/f_b correlates with L_{FIR}, while there is no correlation between f_{FIR}/f_b and L_b, as shown in Figure 5*b*. As seen in Figures 3 and 5*b* the blue luminosities of the galaxies in the bright galaxy sample have a dispersion of ∼1 mag about a mean of $\sim 10^{10}\ L_\odot$ ($M_b \approx -20$ mag) so that larger f_{FIR}/f_b ratios require larger L_{FIR}. The simplest explanation of these results is that the far-infrared and blue luminosity components are basically independent, and the correlation of f_{FIR}/f_b with L_{FIR} is due to increasing infrared emission in the more lumin-

TABLE 1—*Continued*

NAME	RA (1950)	DEC (1950)	F_ν(Jy) 60μm	F_ν(Jy) 100μm	cz km s^{-1}	D Mpc	Log L_{fir} $L_\odot$	m_z[a] mag	Other Name
NGC 4532	12 31 46.3	+ 6 44 38	9.5	15.3	...	20.5	9.97	12.3	UGC 7726
NGC 4535	12 31 48.2	+ 8 28 16	9.3	24.3	...	16.1	9.90	11.1	UGC 7727
NGC 4536	12 31 52.6	+ 2 27 58	32.0	44.1	1824	...	10.83	11.2	
NGC 4559	12 33 29.0	+28 14 2	11.1	28.4	...	13.0	9.79	10.6	
NGC 4565	12 33 52.1	+26 15 32	11.6	48.7	...	13.0	10.01	10.6	
NGC 4568	12 34 2.4	+11 30 54	20.9	47.8	2253	...	10.26	12.5	UGC 7776
NGC 4569	12 34 18.0	+13 26 20	10.6	28.4	...	11.5	9.67	11.8	Arp 76
NGC 4579	12 35 11.6	+12 5 37	6.6	17.4	1805	...	9.83	11.5	M58
NGC 4594	12 37 23.0	−11 21 00	5.6	23.8	1128	...	10.12	9.0	M104
NGC 4605	12 37 48.7	+61 52 52	12.9	30.3	140	...	8.80	10.8	UGC 7831
NGC 4618	12 39 7.8	+41 25 16	6.0	11.2	558	...	8.93	11.5	UGC 7853
NGC 4631	12 39 40.8	+32 49 5	90.0	207.8	613	...	10.09	9.8	Arp 281
NGC 4651	12 41 13.0	+16 39 58	5.5	15.4	...	21.2	9.93	11.3	Arp 189
NGC 4654	12 41 25.2	+13 24 7	13.7	35.2	...	16.2	10.07	11.8	UGC 7902
NGC 4656	12 41 32.0	+32 26 30	7.2	12.3	645	...	8.95	10.6	
NGC 4666	12 42 34.6	− 0 11 20	34.8	77.9	1645	...	10.93	12.0	UGC 7926
NGC 4691	12 45 38.6	− 3 3 36	15.8	21.1	...	23.8	10.28	12.0	
NGC 4710	12 47 9.1	+15 26 13	6.4	13.1	1125	...	9.73	11.6	UGC 7980
MCG+08-23-097	12 48 21.4	+48 12 18	5.4	7.8	8833	...	11.26	16.0	
NGC 4736	12 48 31.7	+41 23 35	70.0	138.7	307	...	9.52	8.7	M94
NGC 4781	12 51 46.3	−10 15 50	8.3	18.0	1265	...	10.10	12.0	
NGC 4783	12 52 15.8	+29 12 36	12.1	27.8	2515	...	10.75	12.3	UGC 8033
NGC 4808	12 53 15.8	+ 4 34 34	7.1	15.0	...	16.1	9.70	12.5	UGC 8054
IC 3908	12 54 4.1	− 7 17 24	8.8	15.9	1052	...	9.36	14.0	
UGC 8058	12 54 4.8	+57 8 38	33.9	29.5	12556	...	12.32	14.1	Mrk 231
NGC 4818	12 54 12.7	− 8 15 18	20.9	25.9	1050	...	9.67	12.0	
NGC 4826	12 54 17.5	+21 57 7	30.2	78.7	414	...	9.24	8.9	M64
NGC 4845	12 55 27.8	+ 1 50 42	9.9	23.5	...	17.4	9.94	12.9	UGC 8078
NGC 4900	12 58 5.8	+ 2 46 12	5.8	12.1	...	17.7	9.69	12.8	UGC 8116
NGC 4922	12 59 1.0	+29 34 59	6.7	6.7	7357	...	11.14	14.2	UGC 8135
MCG+01-33-036	12 59 17.8	+ 4 36 4	5.6	7.4	10852	...	11.42	15.5	
NGC 5005	13 8 37.9	+37 19 26	19.6	59.9	950	...	10.50	10.6	UGC 8256
NGC 5020	13 10 12.5	+12 51 40	5.4	9.9	3354	...	10.52	13.4	UGC 8289
NGC 5033	13 11 9.8	+36 51 25	19.5	53.0	877	...	10.40	10.9	UGC 8307
IC 860	13 12 40.1	+24 52 52	18.4	17.9	3862	...	11.10	14.8	
NGC 5055	13 13 34.8	+42 17 31	45.3	161.0	497	...	10.01	9.7	M63
UGC 8335	13 13 41.3	+62 23 17	11.5	10.2	9356	...	11.60	14.4	VII Zw 506
NGC 5073	13 16 42.5	−14 35 6	9.5	14.8	2715	...	10.54	13.0	
UGC 8387	13 18 19.0	+34 23 49	16.0	23.8	6870	...	11.52	14.8	Arp 193
NGC 5104	13 18 49.2	+ 0 36 14	7.5	12.5	5585	...	11.04	14.5	UGC 8391
NGC 5145	13 23 3.8	+43 31 26	6.7	12.0	1225	...	9.99	13.6	UGC 8439
NGC 5194	13 27 45.4	+47 27 25	121.0	299.0	...	9.3	10.49	8.8	M51
NGC 5195	13 27 52.8	+47 31 30	17.0	20.0	...	9.3	9.47	10.6	UGC 8494
NGC 5218	13 30 26.4	+63 1 26	7.6	14.2	2860	...	10.57	13.1	
NGC 5248	13 35 2.6	+ 9 8 28	18.6	43.9	1156	...	10.22	11.4	UGC 8616
NGC 5256	13 36 14.2	+48 31 52	7.7	11.9	8285	...	11.37	14.1	UGC 8632
NGC 5257/8	13 37 22.1	+ 1 5 13	11.0	18.3	6820	...	11.37	13.7	UGC 8641/5
UGC 8696	13 42 51.6	+56 8 13	24.5	21.2	11400	...	12.10	15.0	Mrk 273
UGC 8739	13 47 1.7	+35 30 14	6.4	14.3	5130	...	11.00	14.7	
NGC 5331	13 49 41.3	+ 2 21 7	6.0	10.2	9950	...	11.43	14.3	VV253

ous galaxies, rather than due to extinction of the visible radiation.

The bright galaxy sample contains no galaxies with low far-infrared luminosities and with f_{FIR}/f_b ratios greater than 10. This lack cannot be a selection effect. At $L_{FIR} \approx 10^{10}\ L_\odot$ the bright galaxy sample includes galaxies to 30 Mpc, certainly a large enough volume to detect such galaxies if they were common. Even at $L_{FIR} \approx 10^9\ L_\odot$, galaxies would be detected to $\sim$10 Mpc. Such galaxies might have very low visible surface brightness and hence not be visible on the POSS. Such galaxies would, if their sizes were similar to the optical size of dwarf irregular galaxies (Gallagher and Hunter 1984), be point sources at distances greater than 6 Mpc, so that they would be contained in the PSC for over 80% of the volume surveyed. Thus the identifications from this subset of the bright galaxy sample, where only one object is not accounted for (see above), preclude a significant contribution of dwarf galaxies. The lack of any visible, faint galaxy counterparts to extended sources also argues against such a class of galaxies being present in the SSSC. The work of Helou (1986*a*) has shown that a very small fraction of known dwarf galaxies have detectable 60 μm emission, and this is at a comparatively low level and usually associated with H II regions in these galaxies.

Seven galaxies in the bright galaxy sample are contained in the blue compact galaxy sample of Thuan and Martin (1981). The average absolute blue magnitude of these seven galaxies is $M_b = -19.9$ mag. The mean far-infrared luminosity of these galaxies is $1.8 \times 10^{10}\ L_\odot$, and their mean ratio of infrared to blue light is 2.5; all of these values are close to the median of the entire sample. Thus the infrared properties of the blue

TABLE 1—*Continued*

NAME	RA (1950)	DEC (1950)	F_ν(Jy) 60μm	F_ν(Jy) 100μm	cz km s^{-1}	D Mpc	Log L_{fir} $L_\odot$	m_z[a] mag	Other Name
NGC 5371	13 53 32.5	+40 42 13	5.7	14.0	2565	...	10.46	11.5	UGC 8846
NGC 5383	13 55 0.2	+42 5 20	5.5	12.9	2282	...	10.35	12.5	UGC 8875
NGC 5394	13 56 25.2	+37 41 38	10.1	11.9	3404	...	10.74	13.9	
NGC 5430	13 59 8.4	+59 34 12	10.9	20.2	2819	...	10.72	13.1	
NGC 5433	14 0 24.0	+32 45 0	7.2	11.1	4278	...	10.81	14.0	UGC 8954
NGC 5427	14 0 48.3	− 5 47 25	9.1	27.1	2565	...	10.70	12.0	Arp 271
NGC 5457	14 1 55.7	+54 33 22	96.7	257.4	...	8.1	10.32	8.7	M101
NGC 5506	14 10 38.9	− 2 58 26	8.8	9.3	1809	...	10.20	13.6	
Zw 247.020	14 17 53.8	+49 27 54	6.5	8.1	7800	...	11.21	15.4	Mrk 1490
NGC 5600	14 21 25.7	+14 51 54	5.9	11.4	2349	...	10.33	11.9	UGC 9220
NGC 5595	14 21 27.1	−16 29 53	8.9	15.8	2691	...	10.53	12.5	
NGC 5597	14 21 41.0	−16 32 10	9.1	15.1	2677	...	10.53	13.0	
NGC 5653	14 28 0.2	+31 26 17	11.5	20.8	3514	...	10.90	12.7	UGC 9318
NGC 5663	14 29 57.4	+ 8 18 0	6.9	12.8	2266	...	10.35	12.6	UGC 9352
NGC 5678	14 30 37.4	+58 8 17	8.9	25.3	1929	...	10.52	12.3	
NGC 5676	14 31 1.2	+49 40 37	10.8	30.6	2104	...	10.67	11.7	UGC 9366
IRAS 1434-14	14 34 52.3	−14 47 24	7.1	7.2	24332	...	12.19	16.7[1]	
NGC 5690	14 35 8.4	+ 2 30 25	6.8	16.1	1750	...	10.24	13.1	
NGC 5713	14 37 37.2	− 0 4 34	20.9	36.9	1900	...	10.69	11.7	UGC 9451
NGC 5719	14 38 22.6	− 0 6 18	8.7	17.1	1480	...	10.18	13.8	UGC 9462
NGC 5728	14 39 39.4	−17 2 42	8.8	14.9	2813	...	10.55	12.5	VV75
NGC 5757	14 44 57.8	−18 52 16	6.4	13.0	2771	...	10.46	12.5	
NGC 5775	14 51 26.9	+ 3 44 38	24.2	45.3	1670	...	10.69	13.0	UGC 9579
UGC 9618	14 54 47.8	+24 48 58	6.8	15.3	10100	...	11.59	14.3	Arp 302
NGC 5792	14 55 46.6	− 0 53 24	9.5	19.1	1930	...	10.40	13.5	UGC 9631
NGC 5793	14 56 39.6	−16 29 53	6.8	9.9	3521	...	10.58	14.0	
UGC 9668	15 0 33.8	+83 43 19	5.4	7.6	3917	...	10.59	13.8	Mrk 839
NGC 5866	15 5 7.2	+55 57 14	5.4	17.0	672	...	9.66	11.1	UGC 9723
NGC 5861	15 6 33.1	−11 7 59	10.9	20.6	1867	...	10.38	12.0	
Zw 049.057	15 10 45.6	+ 7 24 43	23.1	30.6	3528	...	11.12	15.5	
NGC 5900	15 13 17.0	+42 23 35	8.2	16.0	2551	...	10.54	15.0	UGC 9790
NGC 5907	15 14 40.8	+56 29 35	11.2	50.2	666	...	10.16	11.4	UGC 9801
I Zw 107	15 16 19.0	+42 55 41	9.7	9.8	12043	...	11.72	14.9	Mrk 848
NGC 5915	15 18 47.5	−12 54 50	11.3	15.6	2338	...	10.48	12.5	
NGC 5929	15 24 20.6	+41 50 56	9.8	13.3	2600	...	10.55	13.0	UGC 9852
IRAS 1525+36	15 25 3.1	+36 9 0	7.5	5.4	16009	...	11.89	16.2[1]	
NGC 5936	15 27 39.4	+13 9 32	9.3	16.4	4029	...	10.89	13.0	UGC 9867
NGC 5937	15 28 9.8	− 2 39 36	10.5	21.0	2488	...	10.61	13.1	
NGC 5953	15 32 13.4	+15 21 43	11.0	20.1	1983	...	10.46	13.3	Arp 91
UGC 9913	15 32 46.3	+23 40 8	110.1	115.1	5452	...	12.12	14.4	Arp 220
IRAS 1533-05	15 33 32.4	− 5 13 59	5.7	9.6	7800	...	11.20	16.8[1]	
NGC 5962	15 34 13.9	+16 46 16	9.0	21.8	1963	...	10.45	12.2	UGC 9926
NGC 5990	15 43 44.6	+ 2 34 12	10.3	15.4	3809	...	10.84	13.1	UGC 10024
NGC 6015	15 50 39.3	+62 27 27	6.2	10.4	...	16.5	9.60	11.6	
NGC 6052	16 3 2.6	+20 40 34	7.4	9.7	4762	...	10.87	14.1	Arp 209
NGC 6070	16 7 26.0	+00 50 19	7.4	12.9	...	29.6	10.19	13.0	UGC 10230
NGC 6090	16 10 24.0	+52 35 6	6.8	9.6	8733	...	11.35	14.0	UGC 10267
MCG+01-42-088	16 28 27.4	+ 4 11 24	7.4	11.5	7075	...	11.21	14.9	
NGC 6181	16 30 10.1	+19 55 48	9.3	20.3	2379	...	10.57	12.7	

compact galaxies in the sample are indistinguishable from the properties of the sample as a whole. None of these galaxies meet Thuan and Martin's definition of being dwarfs, i.e., having $M_B > -18$ mag.

In Figure 6*a* the 60 μm/100 μm flux density ratio, which is monotonic with color temperature, is plotted versus far-infrared luminosity, while in Figure 6*b* the 60 μm/100 μm flux density ratio is plotted versus blue luminosity. There is a correlation between the color temperature and the far-infrared luminosity in the sense that higher luminosities correspond to higher 60 μm/100 μm color temperatures, while there is clearly no correlation between the far-infrared color temperature and the blue luminosity. Such a correlation has been found previously by Miley, Neugebauer, and Soifer (1985) and Rieke and Lebofsky (1986).

The absence of high-luminosity, cold galaxies from the bright galaxy sample is probably not a selection effect. Cold galaxies of a given far-infrared luminosity will have weaker 60 μm fluxes than do warm galaxies, so the volume within which they can be detected at 60 μm is smaller. This selection effect does not account for the change in color temperature with luminosity and does not appear to be able to account for the observed lack of cold galaxies at high luminosity. The volume searched for galaxies having the median 60 μm/100 μm color of those galaxies with $L_{FIR} \approx 10^{10}\ L_\odot$ is $\sim\frac{2}{3}$ that of those galaxies with median color at $L_{FIR} \approx 10^{12}\ L_\odot$ at the same luminosity. Therefore the lack of detection of any such galaxies cannot be simply a color selection effect, but rather indicates a significant decrease in the space density of galaxies at high luminosities and cold color temperatures. Furthermore,

TABLE 1—*Continued*

NAME	RA (1950)	DEC (1950)	F_ν(Jy) 60μm	F_ν(Jy) 100μm	cz km s^{-1}	D Mpc	Log L_{fir} $L_\odot$	m_z[a] mag	Other Name
NGC 6217	16 35 4.8	+78 18 4	11.0	20.9	1359	...	10.22	12.1	Arp 185
NGC 6285/6	16 57 44.9	+59 0 40	10.2	23.5	5600	...	11.28	14.2	Arp 293
IRAS 1713+53	17 13 14.2	+53 13 52	6.6	7.6	15212	...	11.77	16.1[1]	
NGC 6503	17 49 57.8	+70 9 25	12.4	25.4	51	...	8.97	10.9	UGC 11012
MCG–03-57-017	22 28 42.7	−19 17 31	6.1	10.3	7263	...	11.13	14.5	
IRAS 2249-18	22 49 9.6	−18 8 20	5.6	4.3	22807	...	12.06	16.5[1]	
NGC 7448	22 57 34.8	+15 42 47	8.2	17.9	2192	...	10.33	12.0	Arp 13
NGC 7465	22 59 31.9	+15 41 55	6.8	6.5	1959	...	10.03	13.3	
NGC 7469	23 0 44.6	+ 8 36 18	27.8	34.4	4963	...	11.40	13.0	UGC 12332
NGC 7479	23 2 26.6	+12 3 11	12.4	24.8	2382	...	10.55	11.7	UGC 12343
Zw 453.062	23 2 28.1	+19 16 55	8.0	10.7	7373	...	11.23	15.2	
NGC 7541	23 12 11.5	+ 4 15 40	19.5	39.9	2665	...	10.83	12.7	UGC 12447
Zw 475.056	23 13 31.2	+25 16 48	10.1	12.1	8215	...	11.41	15.0	
NGC 7591	23 15 43.9	+ 6 18 47	8.1	13.1	4964	...	10.92	13.8	UGC 12486
NGC 7592	23 15 47.5	− 4 41 20	8.4	10.4	7314	...	11.21	14.0	
NGC 7625	23 17 59.5	+16 57 4	9.6	18.7	1653	...	10.12	12.8	UGC 12529
NGC 7673	23 25 12.0	+23 18 54	5.5	6.7	3407	...	10.39	12.7	Mrk 325
NGC 7674	23 25 24.7	+ 8 30 14	5.7	8.2	8669	...	11.22	13.6	UGC 12608
NGC 7678	23 25 56.6	+22 8 31	7.5	14.8	3491	...	10.64	12.7	UGC 12614
NGC 7679	23 26 13.9	+ 3 14 13	7.7	9.5	5152	...	10.87	13.2	UGC 12618
NGC 7714	23 33 39.8	+ 1 52 34	11.3	10.8	2805	...	10.51	13.1	UGC 12699
NGC 7771	23 48 52.1	+19 49 55	19.1	38.7	4346	...	11.25	13.1	
Mrk 331	23 48 52.8	+20 18 22	17.6	20.3	5385	...	11.27	14.9	
UGC 12915/4	23 59 7.7	+23 12 58	5.8	14.1	4590	...	10.82	13.2	III Zw 125

[a] Magnitude taken from Zwicky catalogs (Zwicky *et al.* 1961–1968). Note (1) indicates magnitude is blue magnitude, from Sanders *et al.* 1987*a*.

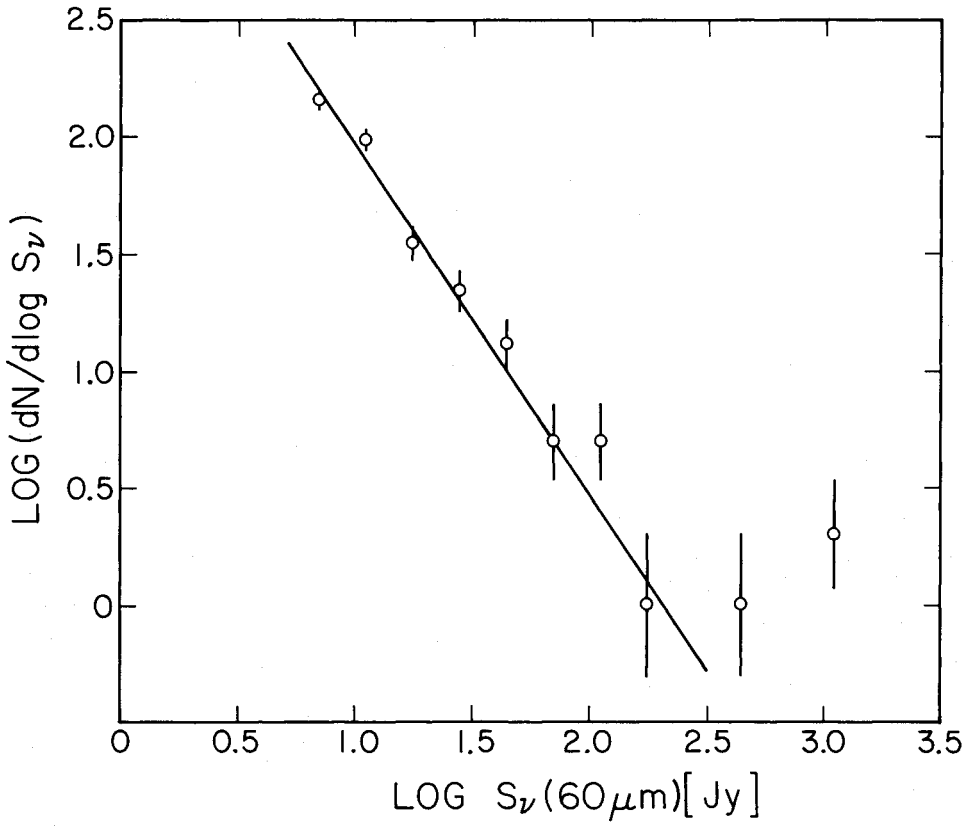

FIG. 1.—Differential number counts of sources plotted vs. flux density for sources in the bright galaxy sample. Each bin includes a range of 1.67 in flux density, while fractional error in each bin is $N^{-1/2}$, where N is number of sources in bin. Line shown is best-fit of data to $N \propto f_\nu^{-3/2}$ power-law number count distribution, and is an acceptable fit to data.

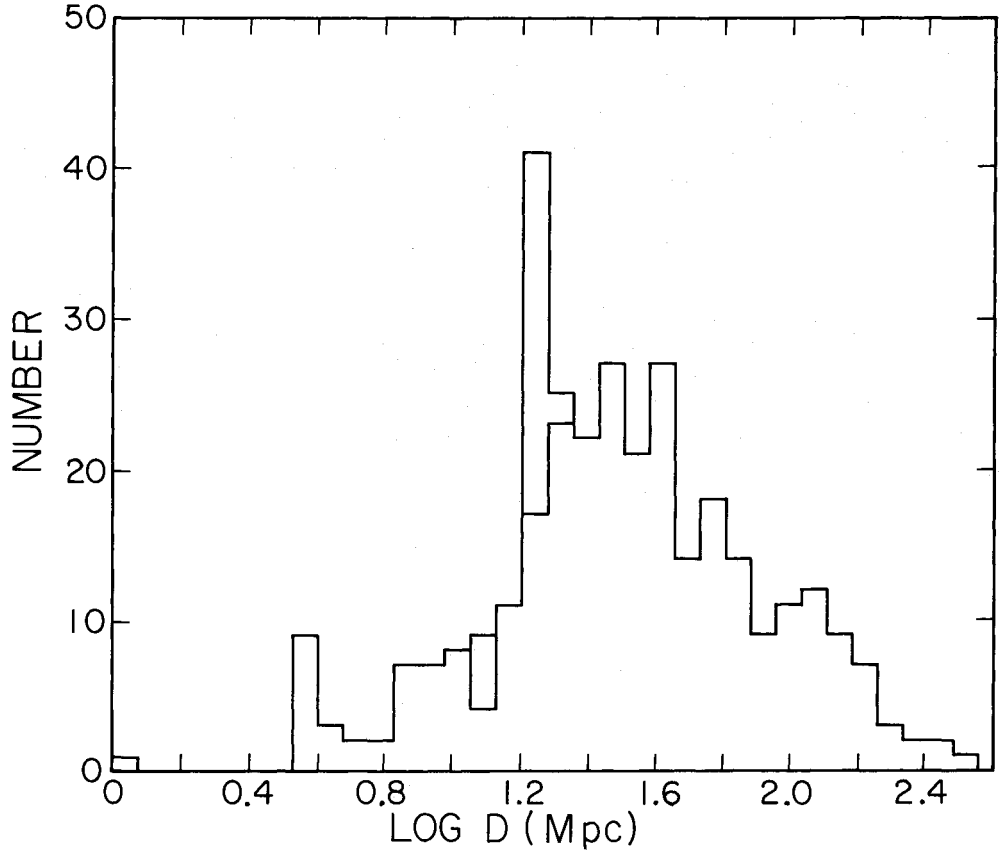

FIG. 2.—Histogram of distances to galaxies in bright galaxy sample, determined as described in text. Lower envelope represents galaxies not associated with Virgo cluster, while histogram above this line includes Virgo cluster galaxies.

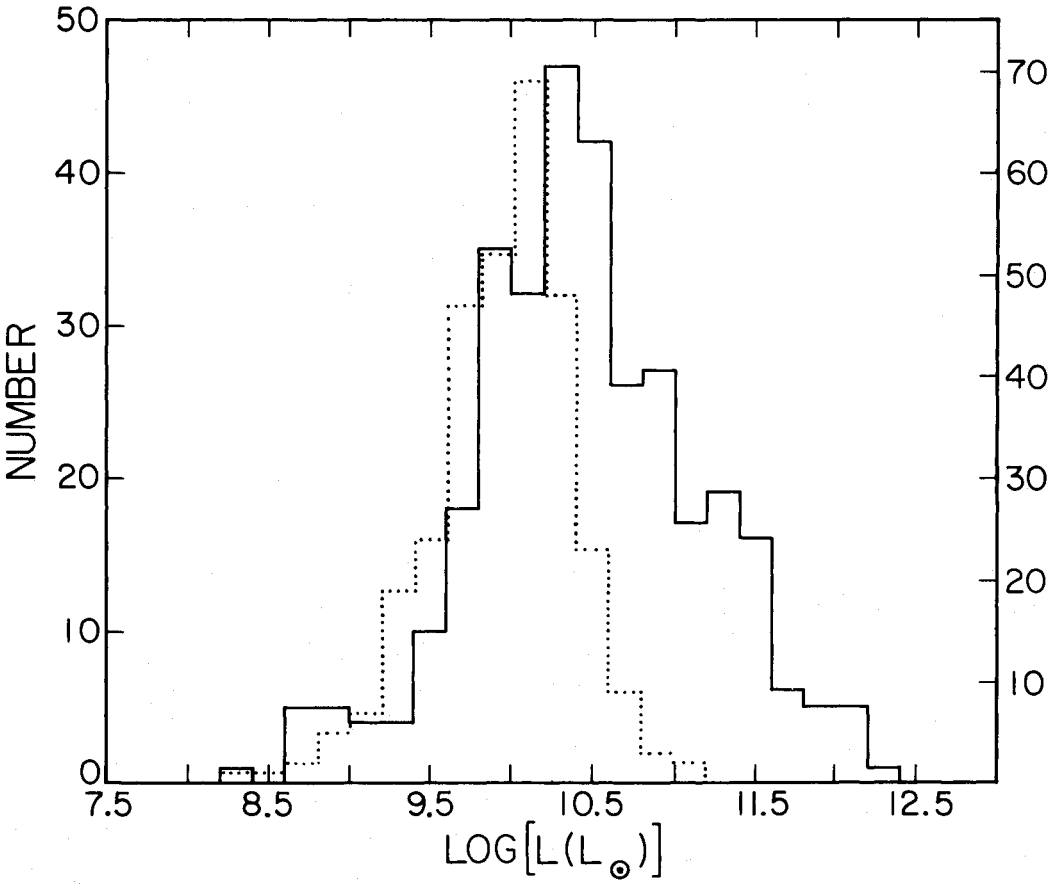

FIG. 3.—Histograms of luminosities of galaxies in bright galaxy sample. Blue luminosity (*dotted line*) is νL_ν(0.43 μm), while far-infrared luminosity (*solid line*) is the luminosity effectively from 40–400 μm (see text). In plot and in text luminosities are given in solar (bolometric) luminosities. Note much narrower distribution of blue compared to far-infrared luminosity.

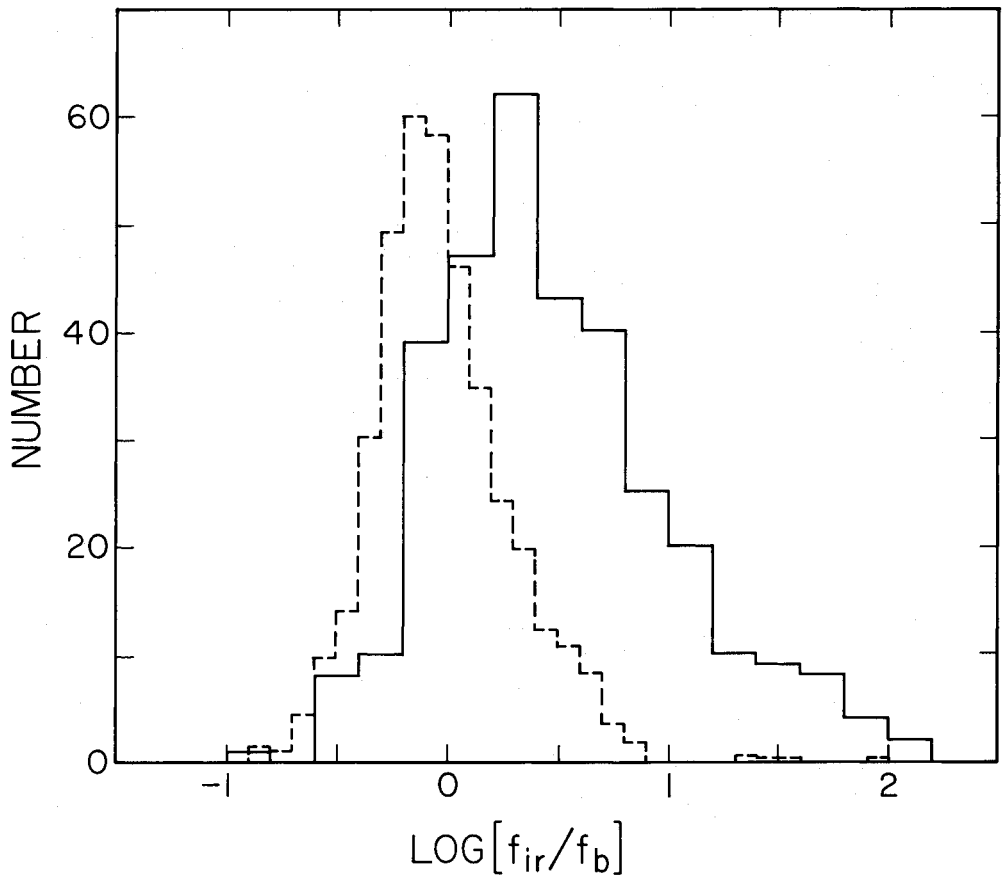

FIG. 4.—Histograms of ratio of far-infrared flux to blue flux for two samples of galaxies detected in *IRAS* survey. Solid line is infrared limited bright galaxy sample, while dashed line is distribution for galaxies in UGC catalog with $m_z < 14.5$ detected in *IRAS* survey (Bothun, Lonsdale, and Rice 1987). Nondetections in UGC catalog have $\log f_{\rm FIR}/f_b < 0$. Histogram for UGC galaxies has been normalized to peak of bright galaxy sample, but contains ~ 10 times more galaxies. One object from UGC galaxies at $\log f_{\rm FIR}/f_b = -1.55$ fell below limits of plot.

a search of the PSC at 100 μm with $b > 50°$ showed no high-luminosity, cold objects that were not contained in the bright galaxy sample.

The apparent maximum 60 μm/100 μm flux density ratio in Figure 6*a*, independent of $L_{\rm FIR}$, implies that the intensity of the radiation field heating the radiating material reaches an effective maximum. The increase of the lower bound of 60 μm/100 μm flux density ratio with increasing luminosity indicates that the minimum radiation field seen by the radiating material is increasing with luminosity.

Lines of constant mass of radiating dust (assuming optically thin dust emission) corresponding to total gas masses (assuming $M_g/M_d = 200$) of 10^8, 10^9, and 10^{10} $M_\odot$ are shown in Figure 6*a*. They show that the amount of material responsible for the far-infrared radiation is roughly comparable to the amount of interstellar matter in normal galaxies, and generally increases with increasing luminosity. Nearly all the galaxies in the bright galaxy sample have masses of dust within this range, with a tendency for the higher luminosity sources to have more radiating material. This range of mass is quite comparable to the amount of mass expected in the interstellar medium of normal spiral galaxies (Sanders *et al.* 1986). Since cold galaxies need more material to produce a given luminosity, the absence of galaxies with high luminosities and low color temperatures may reflect the absence of galaxies having enough interstellar matter to produce such high luminosities without having a generally warmer interstellar medium. Another statement of this is that a luminosity of 10^{12} $L_\odot$ is sufficient to heat the dust corresponding to more than 10^{10} $M_\odot$ of gas and dust to temperatures significantly greater than those found in normal galaxies.

Figure 7 combines the previous two figures, showing the ratio $f_{\rm FIR}/f_b$ plotted versus $f_\nu(60\ \mu{\rm m})/f_\nu(100\ \mu{\rm m})$ for the bright galaxy sample. This plot shows the same general correlation shown previously by de Jong *et al.* (1984) and Soifer *et al.* (1984), where increasing ratio of infrared to blue light is correlated with increasing color temperature. At a given 60 μm/100 μm ratio, the spread in $f_{\rm FIR}/f_b$ is greater in the bright galaxy sample than in the optically selected sample of de Jong *et al.*, while the lower envelope of the $f_{\rm FIR}/f_b$ versus $f_\nu(60\ \mu{\rm m})/f_\nu(100\ \mu{\rm m})$ relation is consistent with the results from the optically selected sample.

VI. SPACE DENSITY OF *IRAS* GALAXIES

a) The 60 μm Luminosity Function

The space density of galaxies in terms of 60 μm luminosity, $\nu L_\nu(60\ \mu{\rm m})$, and the uncertainty in the space density were derived using the expressions

$$\rho = \left(\frac{4\pi}{\Omega}\right)\left(\sum \frac{1}{V_m}\right),$$

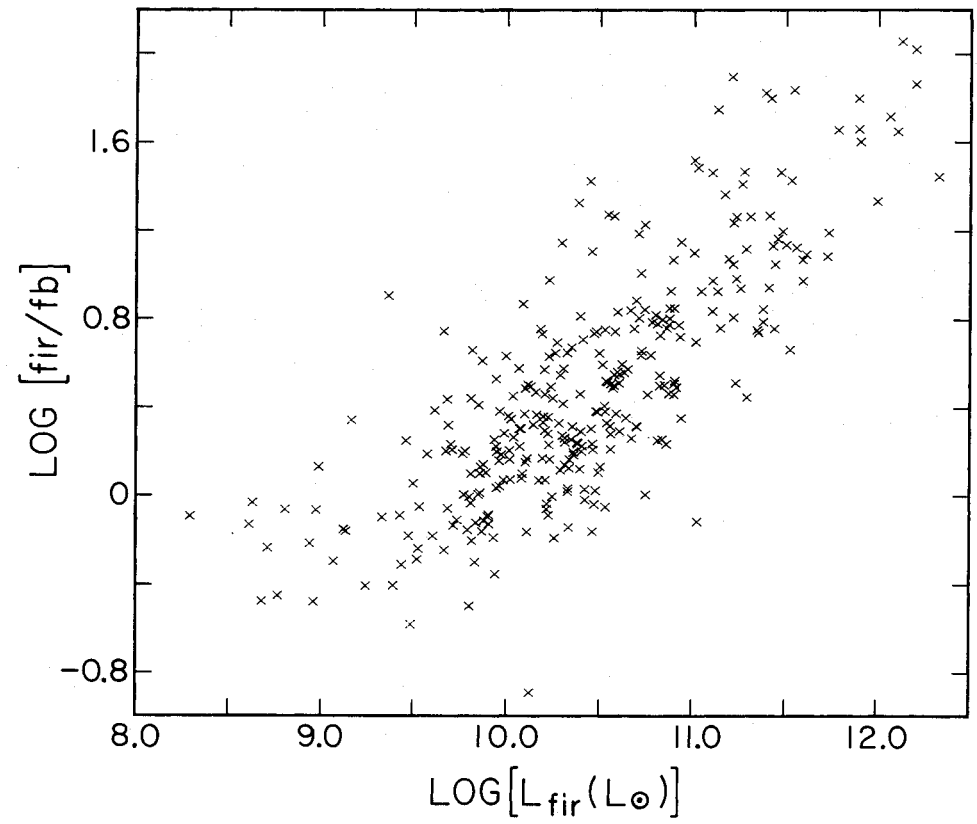

FIG. 5a

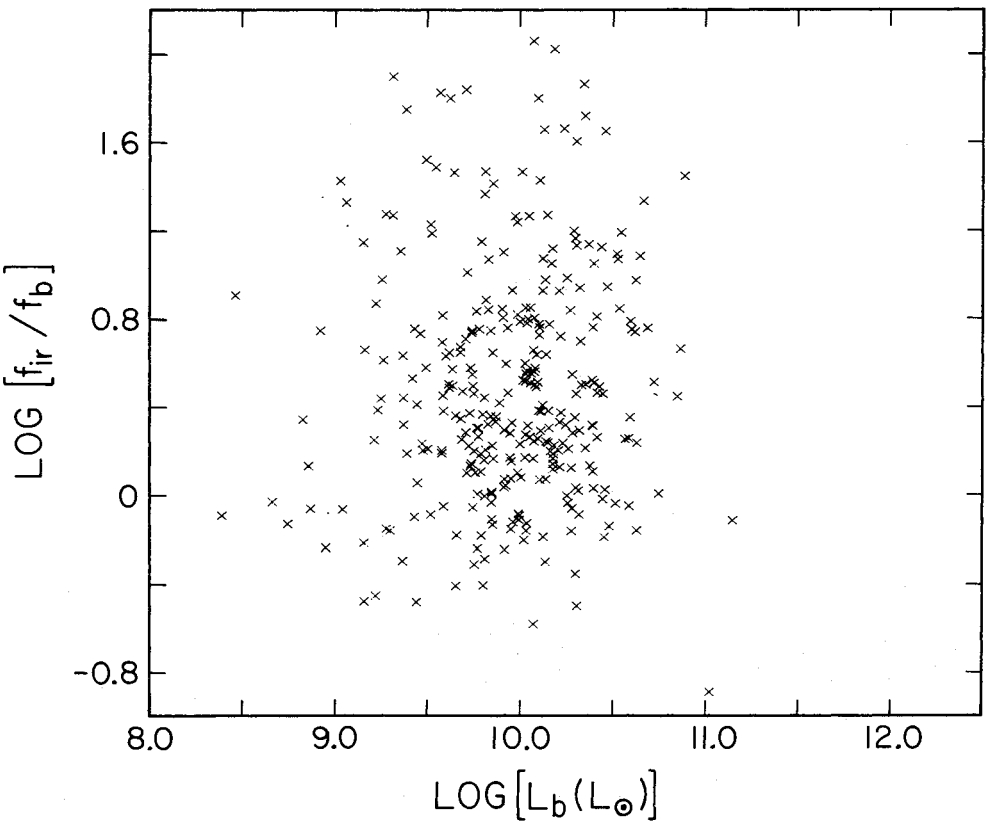

FIG. 5b

FIG. 5.—(*a*) Plot of ratio of far-infrared to blue flux vs. far-infrared luminosity for bright galaxy sample. Increase in average ratio of far-infrared to blue flux is closely linearly proportional to far-infrared luminosity. (*b*) Plot of ratio of far-infrared to blue flux vs. blue luminosity for bright galaxy sample. There is no apparent correlation between these quantities.

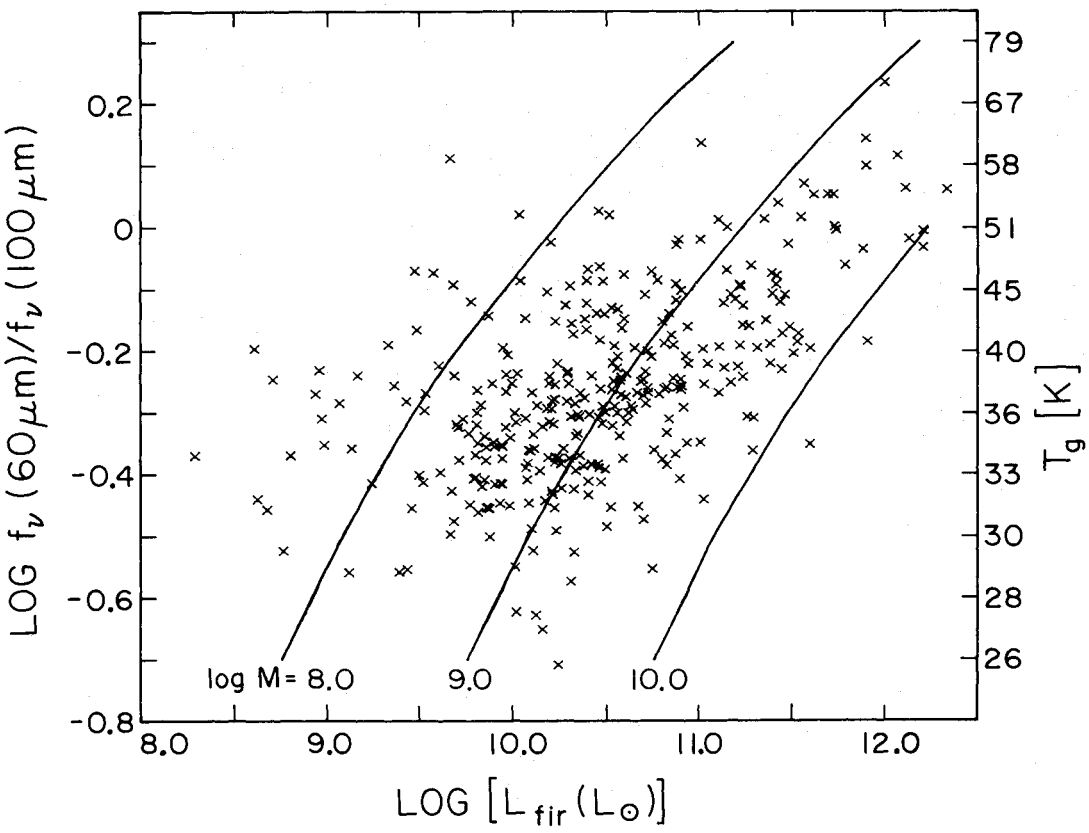

FIG. 6a

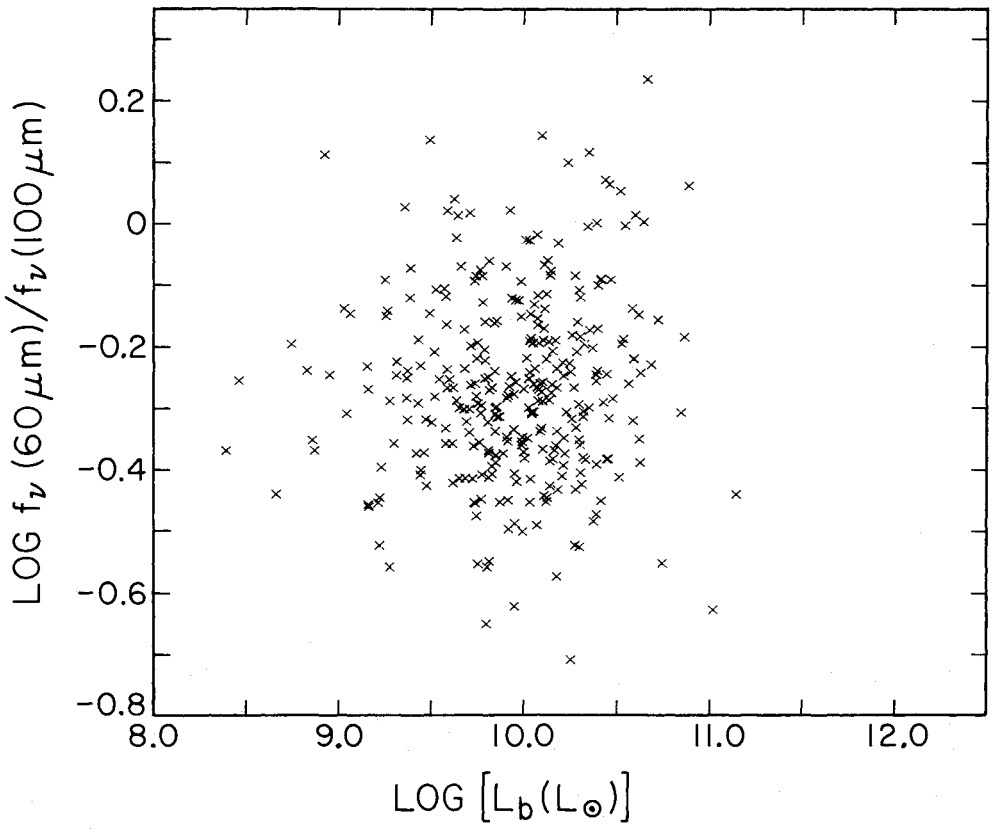

FIG. 6b

FIG. 6.—(*a*) Plot of ratio of 60 μm/100 μm flux densities vs. far-infrared luminosity bright galaxy sample. Ordinate is also shown as grain temperature for grains having emissivity $\epsilon \propto \nu$. Lines of gas mass of 10^8, 10^9, and 10^{10} $M_\odot$ are drawn, where $M_g/M_d = 200$ has been assumed. Dust is assumed to radiate with temperature given by right hand temperature scale, and 100 μm dust opacity is taken from Draine and Lee (1984). (*b*) Plot of ratio of 60 μm/100 μm flux densities vs. blue luminosity for bright galaxy sample. No correlation is apparent between these quantities.

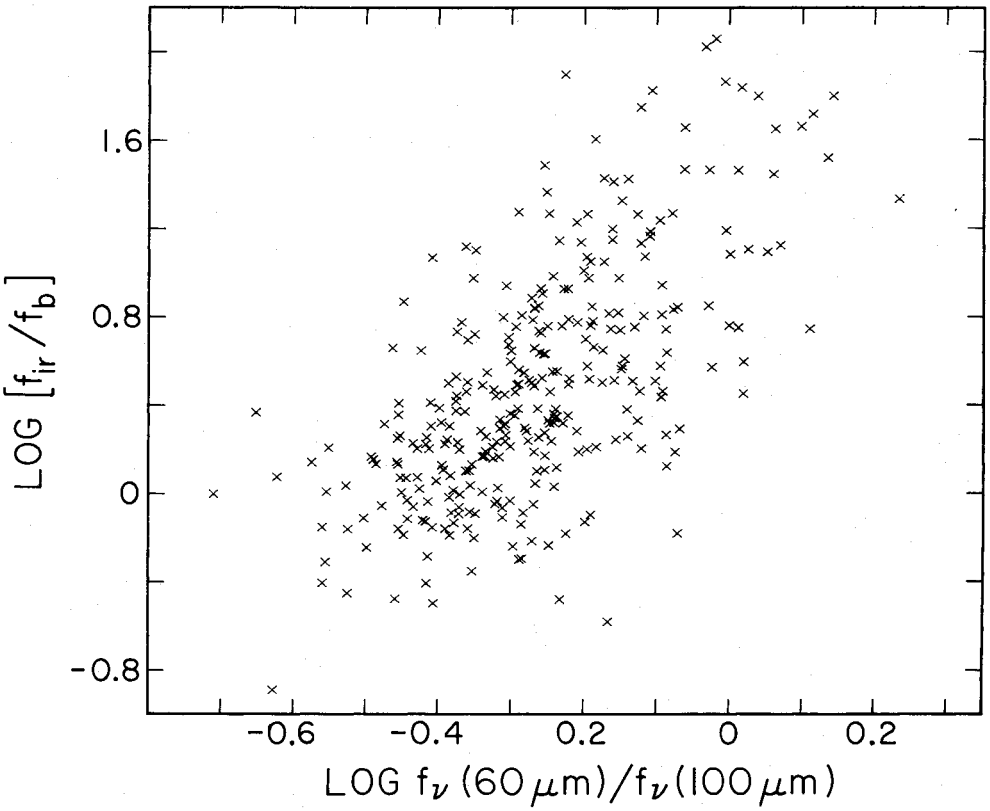

FIG. 7.—Plot of ratio of far-infrared to blue flux vs. 60 μm/100 μm flux density for bright galaxy sample. There is a tendency for higher values of f_{FIR}/f_b to be associated with higher 60 μm/100 μm ratios.

and

$$\sigma_\rho = \left(\frac{4\pi}{\Omega}\right)\left(\sum \frac{1}{V_m^2}\right)^{1/2},$$

where Ω is the solid angle of the survey, and V_m is the maximum volume to which the object could have been detected in the survey, and the summation is over all galaxies in a given luminosity bin (Schmidt 1968).

The more sophisticated estimator of Felton (1976) reduces to the above expression for a uniform flux limit for the survey, as is the case here. Here V_m was individually estimated for each galaxy in the sample. The K correction, determined using a power-law slope (Sandage 1975) defined by the observed 60 μm and 100 μm flux densities, was taken into account in calculating V_m. Since all redshifts are comparatively small, this power law defines the spectrum near 60 μm better than the slope between 25 μm and 60 μm does.

The space densities as a function of luminosity are given in Table 2, along with the number of galaxies in each luminosity bin, the uncertainty in the space density, and the average V/V_m for that bin along with its uncertainty. The quantities are given both including and excluding galaxies deemed to be associated with the Virgo cluster. The luminosity function that excludes

TABLE 2

LUMINOSITY FUNCTION AT 60 MICRONS

	ALL GALAXIES			GALAXIES: VIRGO EXCLUDED		
log L^a ($L_\odot$)	N	ρ (Mpc^{-3} mag^{-1})	V/V_m	N	ρ (Mpc^{-3} mag^{-1})	V/V_m
8.2.....	4	$3.2 \pm 1.7 \times 10^{-2}$	0.50 ± 0.13	...	...	...
8.6.....	8	$1.6 \pm 0.6 \times 10^{-2}$	0.36 ± 0.09	...	...	...
9.0.....	11	$5.6 \pm 1.8 \times 10^{-3}$	0.45 ± 0.08	...	...	...
9.4.....	41	$4.4 \pm 0.7 \times 10^{-3}$	0.59 ± 0.05	23	$2.6 \pm 0.6 \times 10^{-3}$	0.55 ± 0.07
9.8.....	62	$2.1 \pm 0.3 \times 10^{-3}$	0.44 ± 0.03	52	$1.8 \pm 0.3 \times 10^{-3}$	0.47 ± 0.04
10.2.....	78	$6.6 \pm 0.8 \times 10^{-4}$	0.42 ± 0.03	75	$6.3 \pm 0.8 \times 10^{-4}$	0.43 ± 0.03
10.6.....	53	$1.1 \pm 0.2 \times 10^{-4}$	0.45 ± 0.04	...	...	...
11.0.....	29	$1.5 \pm 0.3 \times 10^{-5}$	0.58 ± 0.05	...	...	...
11.4.....	25	$4.0 \pm 0.8 \times 10^{-6}$	0.47 ± 0.06	...	...	...
11.8.....	9	$3.1 \pm 1.1 \times 10^{-7}$	0.46 ± 0.09	...	...	...
12.2.....	4	$4.3 \pm 2.2 \times 10^{-8}$	0.29 ± 0.15	...	...	...

[a] $L(60\ \mu m) = \nu L_\nu(60\ \mu m)$.

the Virgo cluster takes no account of the volume excluded from the sample; this volume is less than 8% of the total surveyed volume in all bins.

In Figure 8 the quantity V/V_m as a function of 60 μm luminosity is plotted. Where appropriate, the V/V_m data with the Virgo galaxies included and excluded are shown. There are no significant deviations from the value of 0.5 expected for a sample that homogeneously fills the volume, with the maximum deviation from the uniform case being for the bin log $[\nu L_\nu(60\ \mu\text{m})] = 10.2$ with V/V_m of 0.43, a 2.5 σ result. For the entire sample, $V/V_m = 0.47 \pm 0.02$, again not significantly different from 0.5. The effect of the Virgo cluster can also be seen in the points where these galaxies are included. In the bins at log $[\nu L_\nu(60\ \mu\text{m})] = 9.4$, 9.8, and 10.2 the inclusion of the Virgo cluster galaxies makes V/V_m differ significantly from 0.5.

Other 60 μm luminosity functions have been derived based on different samples taken from the *IRAS* data (e.g., Lawrence *et al.* 1986; Rieke and Lebofsky 1986; Smith *et al.* 1987). All of these 60 μm luminosity functions are compared with the luminosity function for the bright galaxy sample in Figure 9. All the luminosity functions have been converted to the units adopted here. In the case of the Lawrence *et al.* results, the only conversion necessary was for different Hubble constants. No attempt was made to account for differing value of q_0, since the largest redshifts in the bright galaxy sample are less than $z = 0.1$. For the Smith *et al.* results the only conversions necessary were for the Hubble constant and a different multiplier of $L_\nu(60\ \mu\text{m})$. For the Rieke and Lebofsky sample, the relation $L = 1.6 \times \nu L_\nu(60\ \mu\text{m})$ was adopted based on the distribution of flux ratios presented in their work. As can be seen from Figure 9, the agreement between the luminosity functions derived from different samples is excellent.

While the criteria used to define the bright galaxy sample were based on 60 μm flux density and optical identification, it is interesting to consider whether this sample differs from galaxy samples chosen based on infrared color criteria for studies of the spatial distribution of infrared galaxies (e.g., Yahil, Walker, and Rowan-Robinson 1986; Meiksin and Davis 1986). All of the objects in the bright galaxy sample meet the criteria for inclusion in both of these samples, while neither Yahil, Walker, and Rowan-Robinson nor the Meiksin and Davis samples include objects that would be excluded based on color criteria from the bright galaxy sample. Thus it appears that there are no substantial differences between these samples, and the bright galaxy sample can be used as a fiducial point for fainter, more distant samples of infrared selected galaxies.

Rieke and Lebofsky (1986) have shown that the Schechter (1976) type luminosity function falls below the observed luminosity function at high luminosity. This is also seen in Figure 9. Two power laws fitted to the observed 60 μm luminosity function are also shown in Figure 9. At low luminosities the best-fit power law gives a slope $\rho \sim L^{-0.8}$, while at high luminosities the best-fit slope is $\rho \sim L^{-2.0}$, again in good agreement with the best-fit power law slope of -2.1 estimated by Rieke and Lebofsky. The slope at low luminosity agrees well with the slope for this region of -0.8 derived by Lawrence *et al.* (1986), while at the high-luminosity end the slope is steeper than that

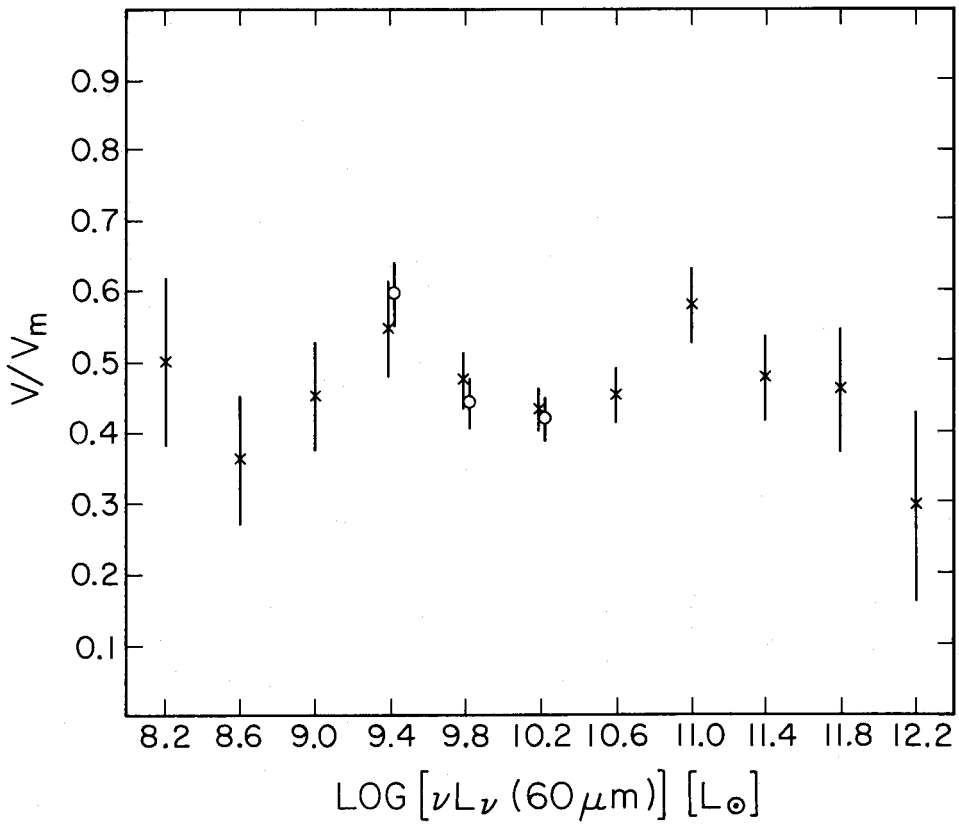

FIG. 8.—Mean V/V_m for the galaxies in bright galaxy sample plotted vs. luminosity of appropriate bin. Crosses represent bins where Virgo cluster galaxies have been excluded, open circles represent all galaxies in those luminosity bins. Only with inclusion of Virgo galaxies are any statistically significant deviations from value of 0.5 expected for galaxies uniformly distributed in volume.

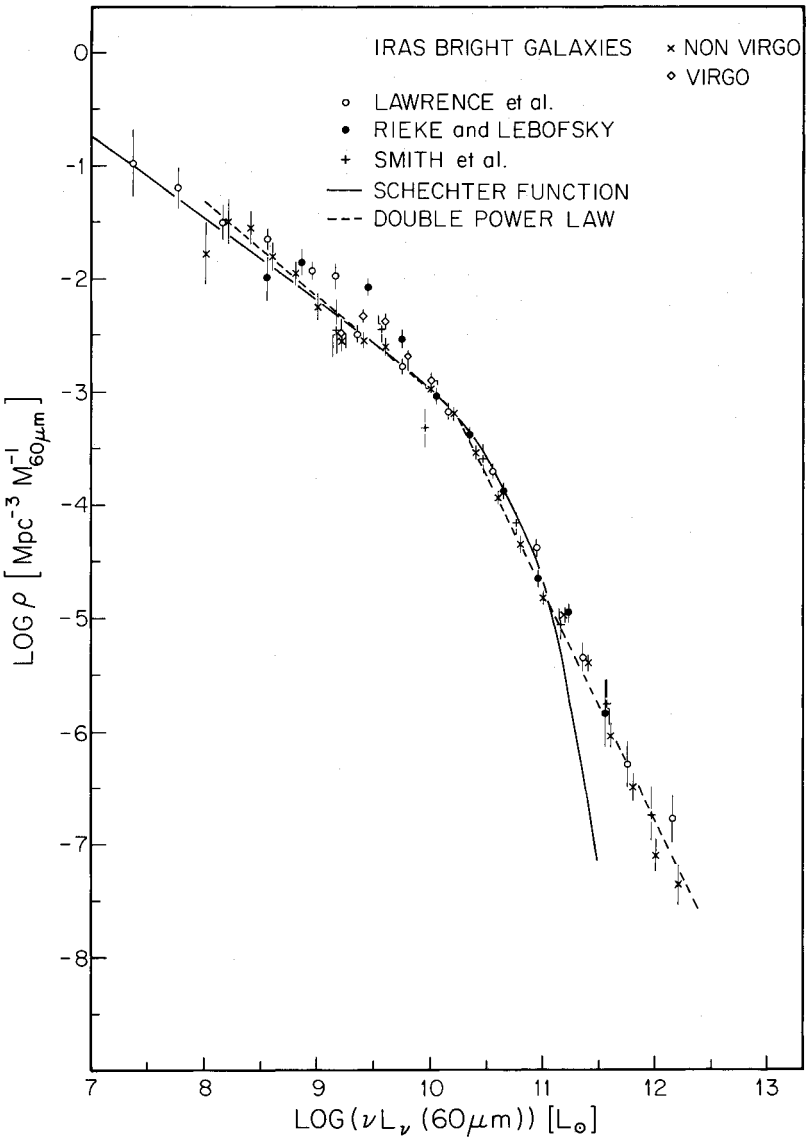

FIG. 9.—The 60 μm luminosity functions from different samples, compared to that derived here for bright galaxy sample. Luminosity functions have been adjusted to same Hubble constant ($H_0 = 75$ km s^{-1} Mpc^{-1}), same definition of luminosity (νL_ν[60 μm]), and bins represent space density in galaxies per Mpc^3 per magnitude interval in luminosity. Otherwise no adjustments have been made to different luminosity functions. Bright galaxy luminosity function is shown excluding Virgo (*crosses*), and three bins, including Virgo galaxies (*open diamonds*). Other luminosity functions shown are from Lawrence *et al.* 1986 (*open circles*), Rieke and Lebofsky 1986 (*filled circles*), and Smith *et al.* 1987 (*plus signs*). Solid line represents a "by eye" fit of a Schechter function to all luminosity functions. Note substantial discrepancy at high luminosity end of luminosity function. Dashed line represents best fit of two power laws to bright galaxy luminosity function.

of -1.7 from Lawrence *et al.*, consistent with the observed space densities in the sample of Lawrence *et al.* being higher at the highest luminosities. The luminosity of the break between the two power laws is $1.7 \times 10^{10}\ L_\odot$; this is the most frequent luminosity seen in this flux-limited sample.

Whether the 60 μm luminosity function can be extrapolated to higher luminosities is quite uncertain. Based on the luminosity function derived above, approximately three objects should have been discovered in the bright galaxy sample with luminosities placing them in the next greater luminosity bin. Clearly the absence of any such examples has no statistical significance, while a handful of fainter, more luminous objects are already known to exist in the *IRAS* survey (e.g., 3C 48 and Mrk 1014; Neugebauer, Soifer, and Miley 1985). Furthermore, two infrared "loud" objects have been found in the luminosity range $10^{13}\ L_\odot$ (Kleinmann and Keel 1987; Vader 1986). The existence of these objects suggests that an extrapolation of the observed luminosity function by an order of magnitude is not unrealistic. However, the extension of the far-infrared luminosity function to such luminosities must await a survey of sufficient numbers of *IRAS* galaxies.

It is tempting to use the different luminosity functions to search for potential evolutionary effects. The largest range in distance is achieved by comparing the bright galaxy luminosity function with that of Lawrence *et al.* (1986), where the completeness limit was 0.85 Jy, and by selecting the highest possible luminosity bin for comparison. Figure 9 shows a suggestion of the luminosity function changing in the expected way if there were an increased density of high-luminosity infrared galaxies in the past. Formally, the increase in density of

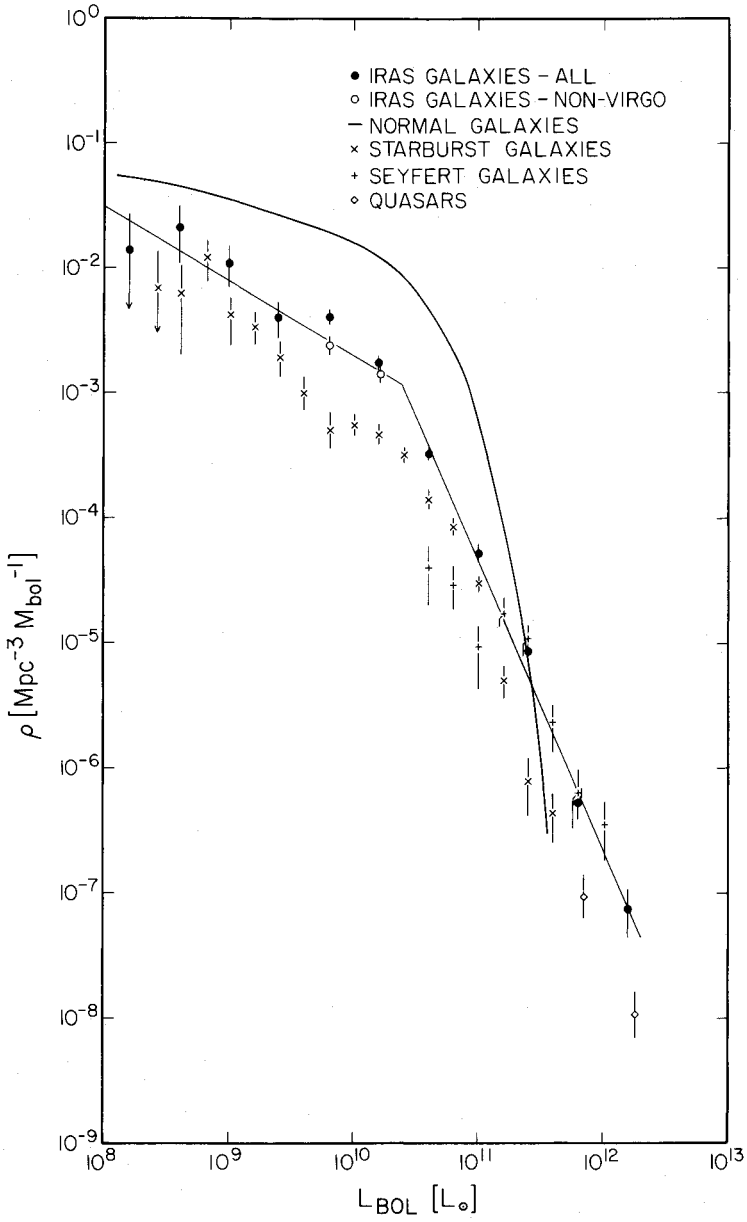

FIG. 10.—Luminosity functions of a variety of classes of extraglactic sources, normalized to same Hubble constant (H_0 = 75 km s^{-1} Mpc^{-1}) and plotted in units of bolometric luminosity. Filled and open circles represent far-infrared luminosity function derived for bright galaxy sample, including and excluding the Virgo cluster respectively. Solid curve represents analytical fit to normal galaxy luminosity function taken from Schechter (1976) that agrees with many observed luminosity functions (Felton, 1977); crosses represent the optically selected starburst galaxies, and plus signs represent the optically selected Seyfert galaxies, both taken from Huchra (1977). Open diamonds represent optically selected quasars taken from Schmidt and Green (1983). Corrections applied to convert from blue luminosity to bolometric luminosity are described in appendix. Straight lines represent best fit of two power laws to bright galaxy luminosity function excluding Virgo galaxies.

galaxies in the range log [νL_ν(60 μm)] = 12.0–12.4 is a factor of ~3. This highly uncertain increase in space density with redshift is consistent with the analysis of the counts of 60 μm sources at the 50 mJy level by Hacking, Condon, and Houck (1987).

b) Comparison with Other Classes of Objects

One goal of the present study is to understand the significance of far-infrared emission in the local universe. This requires comparing the luminosities emitted at different wavelengths by very different classes of objects. In Figure 10, the bolometric luminosity functions of a variety of different classes of extragalactic objects are plotted. The far-infrared luminosity described above has been adopted as the bolometric luminosity for the *IRAS* bright galaxy sample. The total far-infrared luminosities calculated in this way are ~50% greater than the 60 μm luminosities. This ignores an additional contribution of ~25% to the total luminosity from the emission at shorter wavelengths.

Table 3 gives the far-infrared luminosity function. The calculations were done as for the 60 μm space densities; the only difference was the binning by total far-infrared luminosity,

TABLE 3

FAR-INFRARED LUMINOSITY FUNCTION

	ALL GALAXIES		GALAXIES: VIRGO EXCLUDED	
log L_{FIR}[a] ($L_\odot$)	N	ρ (Mpc^{-3} mag^{-1})	N	ρ (Mpc^{-3} mag^{-1})
8.2.....	1	$1.5 \pm 1.5 \times 10^{-2}$	...	...
8.6.....	5	$2.3 \pm 1.1 \times 10^{-2}$	...	...
9.0.....	9	$1.2 \pm 0.4 \times 10^{-2}$	...	...
9.4.....	14	$4.3 \pm 1.3 \times 10^{-3}$	...	...
9.8.....	52	$4.2 \pm 0.6 \times 10^{-3}$	31	$2.3 \pm 0.5 \times 10^{-3}$
10.2.....	79	$1.8 \pm 0.3 \times 10^{-3}$	70	$1.5 \pm 0.2 \times 10^{-3}$
10.6.....	68	$3.5 \pm 0.5 \times 10^{-4}$	67	$3.4 \pm 0.5 \times 10^{-4}$
11.0.....	44	$5.6 \pm 0.9 \times 10^{-5}$	...	...
11.4.....	35	$9.2 \pm 1.7 \times 10^{-6}$	...	...
11.8.....	11	$5.7 \pm 1.8 \times 10^{-7}$	...	...
12.2.....	6	$7.9 \pm 3.4 \times 10^{-8}$	...	...

[a] L_{FIR} is defined in the text.

rather than 60 μm luminosities. The data in Table 3 are used below to compare "bolometric luminosity functions" of different luminosity components in galaxies.

The bright galaxy sample is only strictly complete at 60 μm, and not in a bolometric sense over the entire far-infrared wavelength range. Thus there could be cold or warm objects that are extremely numerous but would not be included in the bright galaxy sample. The PSC was searched using 60 μm/100 μm and 25 μm/60 μm color criteria intended to determine if objects colder or warmer than those selected here might be numerous compared to the bright galaxy sample. While both cold and warm galaxies were found, based on the additional searches of the PSC such objects are likely to comprise less than 25% of the galaxies at a given far-infrared luminosity within a given volume. We conclude that the bright galaxy sample represents a legitimate sample of the local universe in the far-infrared.

For comparison, luminosity functions taken from the literature for "normal galaxies," "starburst galaxies," Seyfert galaxies, and quasars are included in Figure 10. The published luminosity functions are given in terms of M_b, i.e., absolute blue luminosity, so it was necessary to estimate a bolometric correction for each of the classes of objects. The steps taken to derive these bolometric corrections were described in Paper I, but the details are repeated in the Appendix for completeness.

It is important to remember, when comparing the different luminosity functions, that some galaxies can simultaneously be classified in more than one category of object, and are not necessarily evaluated at the same luminosity in each category. Figure 10 should thus be viewed as a comparison of the space density of sources of far-infrared luminosity with that of sources of luminosity that emerge predominantly at shorter wavelengths. For example, the starburst galaxies comprise a subset of the "normal" galaxies, and their luminosity is estimated in a similar way. The bolometric corrections described in the Appendix for these classes of galaxies do not include the far-infrared luminosity emitted by such galaxies (above that in the stellar photospheres). For the Seyferts and quasars, an estimate of the far-infrared luminosity has been included in the calculation of the luminosity, but this is only 10%–15% of the total luminosity of these objects.

One can immediately see from Figure 10 that the emission from infrared bright galaxies represents a significant component of luminosity in the local universe. The infrared galaxies are more numerous by a factor of ~ 3 than Markarian starburst galaxies at $L_{FIR} \lesssim 10^{10} L_\odot$. In the range 10^{10} $L_\odot$–$10^{11} L_\odot$, the densities of the two classes of objects are comparable. For luminosities above $\sim 2 \times 10^{11} L_\odot$ infrared luminous galaxies appear to be the dominant source of luminosity in the local universe, having virtually the same space densities as the Seyferts at the lower end of this range, and a significantly greater space density than quasars at the higher luminosities. A detailed discussion of the spectroscopic and morphological properties of the galaxies in this highest range of infrared luminosities of the bright galaxy sample is in preparation (Sanders *et al.* 1987*a*).

For luminosities below $\sim 2 \times 10^{11} L_\odot$, normal galaxies dominate the space densities in the local universe. From the far-infrared luminosity function the contribution to the luminosity density of the local universe can be estimated. The infrared galaxies with far-infrared luminosities greater than $10^8 L_\odot$ produce $\sim 9 \times 10^7 L_\odot$ Mpc^{-3} in far-infrared emission, with $4 \times 10^7 L_\odot$ Mpc^{-3} being generated in galaxies with far-infrared luminosities greater than $10^{10} L_\odot$. By comparison, the normal galaxies produce a bolometric luminosity density of $\sim 4 \times 10^8 L_\odot$ Mpc^{-3}, where the integrated blue luminosity density taken from Felton (1977) and Yahil, Sandage, and Tammann (1980), corrected to $H_0 = 75$ km s^{-1} Mpc^{-1}, has been corrected by the same bolometric correction as adopted for normal galaxies. Thus the far-infrared luminosity is $\sim 25\%$ of the stellar luminosity of galaxies. Felton and Yahil, Sandage, and Tammann estimate the luminosity density of normal galxies by reducing the absolute scale factor for the local luminosity function to that determined from the number counts at faint magnitudes (see Appendix). There is no evidence that this same factor should be applied to the infrared luminosity function. Indeed, the agreement betwen the luminosity functions of the bright galaxy sample and that of Lawrence *et al.* (1986) suggests that the 60 μm luminosity function remains constant in normalization when the median galaxy distance changes from ~ 30 Mpc to ~ 100 Mpc. Perhaps the absence of elliptical and dwarf galaxies from the infrared selected samples contributes to the more uniform density.

At luminosities greater than $\sim 10^{10} L_\odot$ it is likely that star formation is the dominant form of energy generation in infrared bright galaxies (Becklin 1987), at least until the very highest luminosities. Several authors (Persson and Helou 1986; Helou 1986*b*; Rowan-Robinson and Crawford 1987; de Jong and Brink 1987) have suggested that a significant fraction of the far-infrared luminosity in less active galaxies is recycled stellar radiation not directly associated with star-formation regions. Thus, directly or indirectly, star formation accounts for between 60% and 80% of the far-infrared luminosity generated in the local universe.

The total space density of galaxies with far-infrared luminosities greater than $10^{11} L_\odot$ is $\sim 1.2 \times 10^{-5}$ Mpc^{-3}. Figure 5*a* shows that 85% of these galaxies have blue luminosities greater than $10^{10} L_\odot$. From Christensen (1975), the space density of normal galaxies with $L_0 > 10^{10} L_\odot$ is 3.4×10^{-3} Mpc^{-3}, or $\sim 0.3\%$ of the galaxies with $L_b > 10^{10} L_\odot$ have $L_{FIR} > 10^{11} L_\odot$. If the infrared bright phase has a lifetime t_{IR} and the optical phase has a lifetime t_b then the fraction of galaxies that have undergone such an infrared active phase is $0.003 \times t_b/t_{IR}$. If the overall normalization of the optical luminosity function is reduced by a factor of 2.3 (Felton 1977) while the far-infrared luminosity function remains constant, as suggested in Figure 9, then the fraction of galaxies undergoing this

phase become $0.007 \times t_b/t_{IR}$. As noted in Paper I, if $t_b \sim 10^{10}$ yr and the infrared bright phase is a nonrecurring starburst phase with $t_{IR} < 10^8$ yr (Rieke *et al.* 1980; Gerhz, Sramek, and Weedman 1983), then a significant fraction, perhaps more than 50%, of galaxies with $L_b > 10^{10}\ L_\odot$ must have undergone such an infrared active period. If t_b is as small as 10^9 yr and t_{IR} is $\sim 10^8$ yr, then almost 10% of such galaxies could undergo such a phase.

VII. SUMMARY

From a complete sample of the brightest galaxies detected at 60 μm in the *IRAS* all-sky survey, we have found the following:

1. Far-infrared emission is a significant luminosity component in the local universe, representing 25% of the luminosity emitted by stars in the same volume. Above $10^{11}\ L_\odot$ the infrared luminous galaxies are the dominant population of objects in the universe, being as numerous as the Seyfert galaxies, and more numerous than quasars at higher luminosities.
2. The infrared luminosity appears to be independent of the optical luminosity of galaxies. Most infrared bright galaxies appear to require much, if not all, of their interstellar matter to be contributing to the observed infrared luminosity.
3. Approximately 60%–80% of the far-infrared luminosity of the local universe can be attributed, directly or indirectly, to recent or ongoing star formation.

It is a pleasure to thank members of the IPAC staff for assistance in assembling *IRAS* data, our night assistants at Palomar, Juan Carasco and Skip Staples, for assistance in obtaining the optical spectra and optical photometry, and George Helou, Paul Schechter, and Jeremy Mould for illuminating conversations. This research was supported in part by NASA through the *IRAS* Extended Mission program, and in part by the NSF. G. E. D. is supported by NASA contract NAS5-25451. B. F. M. is supported in part by the Natural Sciences and Engineering Research Council of Canada and by the Canada Council through a Killam Fellowship. This is contribution No. 4427 of the Division of Geological and Planetary Sciences.

APPENDIX

CONVERSION OF LUMINOSITY FUNCTIONS TO BOLOMETRIC LUMINOSITIES

Nearly all of the luminosity functions derived for classes of extragalactic objects are given in units of M_B. Since the comparison of the far-infrared luminous galaxies with other classes of extragalactic objects requires measuring in comparable units of luminosity, and blue luminosity is not applicable to the infrared luminous galaxies, bolometric luminosity has been selected for comparison of the various luminosity functions.

Felton (1977) has discussed nine optical luminosity functions derived for nearby galaxies, and has concluded that all but one agree. The analytic form of this function formulated by Schechter (1976) is a good fit to these data, and is adopted here as the optical luminosity function of the normal galaxies. Felton has suggested that the local luminosity function for normal galaxies is too high by a factor of ~ 2.3 when comparing the number counts of galaxies at fainter magnitudes with those predicted from the local luminosity function. Since the *IRAS* bright galaxy luminosity function has been derived over roughly the same distances as the normal galaxy luminosity function, no adjustment has been made in the normalization of the normal galaxy luminosity function. An average $B-V$ color for the normal galaxies was taken as 0.8 mag, and a bolometric correction of 0.9 mag was adopted. This bolometric correction is consistent with the $V-K$ colors of typical galaxies (Aaronson 1977; Johnson 1966).

The non-Seyfert Markarian galaxies represent the most complete sample of optically selected starburst galaxies (Bohuski, Fairall, and Weedman 1978) and the luminosity function for these galaxies was taken from the work of Huchra (1977). A mean $B-V$ color of 0.5 mag and a bolometric correction of 1.2 mag are adopted for these galaxies (Huchra 1977; Balzano 1983). This correction includes contributions for the photospheres of late-type and hot stars in these galaxies.

The luminosity function for Seyfert galaxies, assumed to be characterized by the luminosity function for the Markarian Seyferts, was taken from Huchra (1977), while the luminosity function for the quasars was taken from Schmidt and Green (1983). The bolometric correction for both of these classes of objects was assumed to be the same and was estimated as $9 \times \nu L_\nu(0.43\ \mu\text{m})$. This was derived by assuming a three-step power-law flux distribution, where the slope ($f_\nu \approx \nu^\alpha$) was taken as -1 for 3×10^{12}–3×10^{14} Hz, -0.5 for 3×10^{14}–3×10^{15} Hz, and -1.5 for 3×10^{15}–3×10^{16} Hz (Malkan and Sargent 1982; Malkan 1983; Elvis *et al.* 1986; O'Dell, Scott, and Stein 1986). A comparison of this approximation with the integrated energy distributions of a variety of AGNS from 0.1 to 100 μm (Edelson and Malkan 1986) indicates that it represents the total bolometric luminosity of these objects to within 30%.

REFERENCES

Aaronson, M. 1977, Ph.D. thesis, Harvard University.
Aaronson, M. *et al.* 1982*a*, *Ap. J. Suppl.*, **50**, 241.
Aaronson, M., Huchra, J., Mould, J., Schechter, P. L., and Tully, R. B. 1982*b*, *Ap. J.*, **258**, 64.
Aaronson, M., and Mould, J. 1983, *Ap. J.*, **265**, 1.
Allen, C. W. 1973, *Astrophysical Quantities* 3d ed.; (London: Athlone).
Balzano, V. 1983, *Ap. J.*, **268**, 602.
Becklin, E. E. 1987, in *Star Formation Galaxies*, ed. C. J. Persson (Washington, DC: US Government Printing Office).
Bohuski, P. J., Fairall, A. P., and Weedman, D. W. 1978, *Ap. J.*, **221**, 776.
Bothun, G., Lonsdale, C. J., and Rice, W. L. 1987, in preparation.
Cataloged Galaxies and Quasars Observed in the IRAS Survey. 1985, prepared by C. J. Lonsdale, G. Helou, J. C. Good, and W. L. Rice (Pasadena: Jet Propulsion Laboratory D-1932).
Chester, T. J. 1986, in *Light on Dark Matter*, ed. F. Israel (Dordrecht: Reidel), p. 3.
Christensen, C. G. 1975, *A.J.*, **80**, 282.
de Jong, T., and Brink, K. 1987, in *Star Formation in Galaxies*, ed. C. J. Persson (Washington, DC: US Government Printing Office), in press.
de Jong., *et al.* 1984, *Ap. J.* (*Letters*), **278**, L67.
de Vaucouleurs, G., de Vaucouleurs, A., and Corwin, H. 1976, *Second Reference Catalogue of Bright Galaxies* (Austin: University of Texas Press).
Draine, B. T., and Lee, H. M. 1984, *Ap. J.*, **258**, 111.
Edelson, R., and Malkan, M. 1986, *Ap. J.*, **308**, 59.
Elvis, M., Green, R. F., Bechtold, J., Schmidt, M., Neugebauer, G., Soifer, B. T., Matthews, K., and Fabbiano, G. 1986, *Ap. J.*, **310**, 291.
Felten, J. E. 1976, *Ap. J.*, **207**, 700.
———. 1977, *A.J.*, **82**, 861.

Gallagher, J. S., and Hunter, D. A. 1984, *Ann. Rev. Astr. Ap.*, **22**, 37.
Gehrz, R. D., Sramek, R. A., and Weedman, D. W. 1983, *Ap. J.*, **267**, 551.
Hacking, P., Condon, J., and Houck, J. R. 1987, *Ap. J.*, submitted.
Helou, G. 1986*a*, in *Workshop on Star-Forming Dwarf Galaxies*, ed. D. Knuth, T. X. Thuan, and J. Trans Thanh Van, (Gif sur Yvette: Editions Frontiers), p. 1.
———. 1986*b*, *Ap. J. (Letters)*, **311**, L33.
Huchra, J. 1977, *Ap. J. Suppl.*, **35**, 171.
Huchra, J., Davis, M., Latham, D., and Tonry, J. 1983, *Ap. J. Suppl.*, **52**, 89.
IRAS Catalogs and Atlases Explanatory Supplement. 1985, ed. C. A. Beichman, G. Neugebauer, H. J. Habing, P. E. Clegg, and T. J. Chester, (Washington, DC: US Government Printing Office).
IRAS Catalogs and Atlases: Point Source Catalog. 1985 (Washington, DC: US Government Printing Office).
IRAS Catalogs and Atlases: Small Scale Structure Catalog. 1986, prepared by G. Helou and D. Walker (Washington, DC: US Government Printing Office).
IRAS Catalogs and Atlases: Introduction to the Small Scale Structure Catalog. 1986, ed. G. Helou, (Washington, DC: US Government Printing Office).
Johnson, H. L. 1966, *Ann. Rev. Astr. Ap.*, **4**, 193.
Kirschner, R. P., Oemler, A., and Schechter, P. L. 1978, *A.J.*, **83**, 1549.
Kleinmann, S., and Keel, W. 1987, in *Star Formation in Galaxies*, ed. C. J. Persson, (Washington, DC: US Government Printing Office), in press.
Lawrence, A., Walker, D., Rowan-Robinson, M., Leech, K. J., and Penston, M. V. 1986, *M.N.R.A.S.*, **219**, 687.
Low, F. J., *et al.* 1984, *Ap. J.*, **278**, L19.
Malkan, M. 1983, *Ap. J.*, **268**, 582.
Malkan, M., and Sargent, W. L. W. 1982, *Ap. J.*, **25**, 22.
Meiksin, A., and Davis, M. 1986, *A.J.*, **91**, 191.
Miley, G., Neugebauer, G., and Soifer, B. T. 1985, *Ap. J. (Letters)*, **293**, L11.
Neugebauer, G., Soifer, B. T., and Miley, G. 1985, *Ap. J. (Letters)*, **295**, L27.
Ney, E. P., *et al.* 1975, *Ap. J. (Letters)*, **198**, L129.
Nilson, P. 1973, *Uppsala General Catalog of Galaxies*, Vol. **1**, (Uppsala: Uppsala Offset Center).
O'Dell, S. L., Scott, H. A., and Stein, W. A. 1986, preprint.
Oke, J. B., and Gunn, J. E. 1982, *Pub. A.S.P.*, **94**, 586.
Palumbo, G. G. C., Tanzella-Nitta, G., and Vettolani, G. 1983, *Catalog of Radial Velocities of Galaxies* (New York: Gordon & Breach).
Persson, C. J., and Helou, G. 1986, *Ap. J.*, **314**, 513.
Rice, W. L., Lonsdale, C. J., Soifer, B. T., Neugebauer, G., and Kopan, E. L. 1987, *Ap. J. Suppl.*, in preparation.
Rieke, G. H., and Lebofsky, M. 1986, *Ap. J.*, **304**, 326.
Rieke, G. H., Lebofsky, M. J., Thompson, R. I., Low, F. J., and Tokunaga, A. T. 1980, *Ap. J.*, **238**, 24.
Rowan-Robinson, M., and Crawford, J. 1987, in *Star Formation in Galaxies*, ed. C. J. Persson (Washington, DC: US Government Printing Office), in press.
Sandage, A. 1975, in *Galaxies and the Universe*, ed. A. Sandage, M. Sandage, and J. Kristian (Chicago: University of Chicago Press), p. 761.
Sandage, A., and Tammann, G. A. 1981, *A Revised Shapely-Ames Catalog of Bright Galaxies* (Washington, DC: Carnegie Institute).
Sanders, D. B., Scoville, N. Z., Young, J. S., Soifer, B. T., Schloerb, F. P., Rice, W. L., and Danielson, G. E. 1986, *Ap. J.*, (*Letters*), **305**, L45.
Sanders, D. B., *et al.* 1987*a*, in preparation.
———. 1987*b*, in preparation.
Schechter, P. 1976, *Ap. J.*, **203**, 297.
Schmidt, M. 1968, *Ap. J.*, **151**, 393.
Schmidt, M., and Green, R. 1983, *Ap. J.*, **269**, 352.
Smith, B. J., Kleinmann, S. G., Huchra, J. P., and Low, F. J. 1987, in *Star Formation in Galaxies*, ed. C. J. Persson, (Washington, DC: US Government Printing Office), in press.
Soifer, B. T., *et al.* 1984, *Ap. J. (Letters)*, **278**, L71.
Soifer, B. T., Sanders, D. B., Neugebauer, G., Danielson, G. E., Lonsdale, C. J., Madore, B. F., and Persson, S. E. 1986, *Ap. J. (Letters)*, **303**, L41 (Paper I).
Thuan, T. X., and Martin, G. E. 1981, *Ap. J.*, **247**, 823.
Vader, J. P. 1986, *IAU Circ.* No. 4265.
Yahil, A., Walker, D., and Rowan-Robinson, M. 1986, *Ap. J. (Letters)*, **301**, L1.
Yahil, A., Sandage, A. R., and Tammann, G. A. 1980, *Ap. J.*, **242**, 448.
Zwicky, F. *et al.* 1961–1968, *Catalog of Galaxies and Clusters of Galaxies* (Pasadena: California Institute of Technology).

G. E. DANIELSON: Palomar Observatory and Division of Geology and Planetary Science, California Institute of Technology, Mudd 170-25, Pasadena, CA 91125

J. ELIAS, B. F. MADORE, G. NEUGEBAUER, D. B. SANDERS, and B. T. SOFIER: California Institute of Technology, Downs 320-47, Pasadena, CA 91125

CAROL J. LONSDALE, and W. L. RICE: IPAC, Mail Code 100-22, California Institute of Technology, Pasadena, CA 91125